ISSN 1882-3440

TECHNOLOGY DEVELOPMENT CENTER NEWS

NATIONAL INSTITUTE OF INFORMATION AND COMMUNICATIONS TECHNOLOGY
Serial No. 31 September 2010

CONTENTS

The 9th NICT IVS-TDC Symposium 1
Ryuichi Ichikawa

Proceedings of the 9th NICT IVS TDC Symposium (Kashima, March 12, 2010)

Current status of development of a transportable and compact VLBI system by NICT and GSI 2
Atsutoshi Ishii, Ryuichi Ichikawa, Hiroshi Takiguchi, Kazuhiro Takefuji, Hideki Ujihara, Yasuhiro Koyama, Tetsuro Kondo, Shinobu Kurihara, Yuji Miura, Shigeru Matsuzaka and Daisuke Tanimoto

Current Status of Next Generation A/D Sampler ADS3000+ 6
Kazuhiro Takefuji, Masanori Tsutsumi, Hiroshi Takeuchi and Yasuhiro Koyama

GPU based GNSS software receivers - status quo and plans 10
Thomas Hobiger, Tadahiro Gotoh, Jun Amagai, Tetsuro Kondo and Yasuhiro Koyama

Automated processing of VLBI experiments with c5++ 14
Thomas Hobiger, Tadahiro Gotoh, Toshimichi Otsubo, Toshihiro Kubooka, Mamoru Sekido, Hiroshi Takiguchi and Hiroshi Takeuchi

UTC(NICT) signal transfer system using optical fibers 17
Miho Fujieda, Motohiro Kumagai, Shigeo Nagano and Tadahiro Gotoh

VLBI Measurements for Frequency Transfer 21
Hiroshi Takiguchi, Yasuhiro Koyama, Ryuichi Ichikawa, Tadahiro Gotoh, Atsutoshi Ishii, Thomas Hobiger and Mizuhiko Hosokawa

Kashima RAy-Tracing Service: KARATS 25
ICHIKAWA Ryuichi, Thomas HOBIGER, HASEGAWA Shingo, TSUTSUMI Masanori, KOYAMA Yasuhiro and KONDO Tetsuro

The 9th NICT IVS-TDC Symposium

ICHIKAWA Ryuichi[1] (*richi@nict.go.jp*)

[1] *Kashima Space Research Center, National Institute of Information and Communications Technology, 893-1 Hirai, Kashima, Ibaraki 314-8501, Japan*

As one of the Technical Development Centers (TDC) of IVS (International VLBI Service for Geodesy and Astrometry), Kashima Space Research Center (KSRC) of National Institute of Information and Communications (NICT) hosted the 9th IVS-TDC Symposium on March 12, 2010 at the KSRC. In this annual symposium we focused on the most recent research and developments related with the VLBI technology. In total, 15 oral and 6 poster papers were presented by researchers from Geograhical Survey Institute, National Astronomical Observatory, Kagoshima University, Yokohama National University and NICT. This volume is the proceedings of the symposium and its includes 8 papers which covered various range of the VLBI study field, i.e. developments of the compact VLBI system and its first geodetic results, development of the digital backend system, time transfer experiment, Korean VLBI activities, development of new VLBI analysis software, ultra rapid UT1-UTC experiment, and development of RFI mitigation. The materials of these presentations are available on the web at **http://www2.nict.go.jp/w/w114/stmp/ivstdc/sympo100312/tdcsympo9.html** (in Japanese).

Figure 1. The symposium participants.

Figure 2. The state of the symposium.

Current status of development of a transportable and compact VLBI system by NICT and GSI

Atsutoshi Ishii[1,2] (*a_ishii@aes.co.jp*), **Ryuichi Ichikawa**[2], **Hiroshi Takiguchi**[2], **Kazuhiro Takefuji**[2], **Hideki Ujihara**[2], **Yasuhiro Koyama**[2], **Tetsuro Kondo**[2], **Shinobu Kurihara**[3], **Yuji Miura**[3], **Shigeru Matsuzaka**[3], and **Daisuke Tanimoto**[1]

[1]*Advance Engineering Services Co., Ltd*
1-6-1 Takezono, Tsukuba, Ibaraki,
305-0032, Japan
[2]*Space-Time Standards Group,*
Kashima Space Research Center,
National Institute of Information and Communications Technology,
893-1 Hirai, Kashima, Ibaraki,
314-8501, Japan
[3]*Geospatial Information Authority of Japan (former Geographical Survey Institute, GSI),*
1 Kitasato, Tsukuba, Ibaraki,
305-0811, Japan

Abstract: MARBLE (Multiple Antenna Radio-interferometer for Baseline Length Evaluation) is under development by NICT and GSI. The main part of MARBLE is a transportable VLBI system with compact antenna. The aim of this system is to provide precise baseline length about ∼10 km for calibration baselines. The calibration baselines are used to check and validate surveying instruments such as GPS receiver and EDM (Electronic-optical Distance Meter). It is necessary to examine the calibration baselines regularly to keep the quality of validation. VLBI technique can examine and evaluate the calibration baselines.

On the other hand, the following roles are expected of a compact VLBI antenna on VLBI2010 project. In order to achieve the challenging measurement precision of VLBI2010, it is well known that to deal with the problem of thermal and gravitational deformation of the antenna is necessary. One of a promising approach has been suggested is connected-element interferometry between a compact antenna and the VLBI2010 antenna. By measuring repeatedly the baseline between the small stable antenna and the VLBI2010 antenna, the deformation of the primary antenna can be measured and the thermal and the gravitational models of the primary antenna will be able to be constructed.

We made two prototypes of transportable and compact VLBI system from 2007 to 2009. We performed VLBI experiments using theses prototypes and got a baseline length between the two prototypes. The formal error of the measured baseline length was 2.7 mm. We expect that a error of baseline length measurement will be reduced by using a high-speed A/D sampler.

1. Introduction

We are developing a transportable and compact VLBI system. One of the purposes of the development is to measure accurately the baseline length of about 10 km. Geospatial Information Authority of Japan (former Geographical Survey Institute, GSI) has a calibration baseline of 10 km to calibrate and validate surveying instruments for public purpose. These surveying instruments are GPS receiver and EDM (Electronic-optical Distance Meter). To keep the quality of the calibration, the calibration baseline has to be examined regularly. However, the calibration baseline have been examined only by GPS receiver until now. Since this approach cannot know the systematic error, the examination by another technique is required. VLBI technique can give an independent measurement the calibration baseline to know the systematic error. To achieve the purpose, we made the following ideas. The geodetic VLBI system has pair of compact VLBI stations with small antennas and a reference VLBI station with a large aperture antenna (figure 1). These small VLBI antennas are placed at intervals of about 10 km. We can obtain the time delay between small antennas by two time delays between the large antenna and small antennas, even if we do not obtain the delay time between small antennas directly. The baseline length of 10 km can be estimated by the indirect time delay. One of the advantages of this idea is not to have to get time delay between small antennas. Another advantage is that the comparison between the VLBI measurement and the GPS measurement is easy, because we only compare the reference point of a small VLBI antenna with the reference point of the GPS antenna. We don't need to compare the reference point of a large VLBI antenna with the GPS reference point. We call this idea '**M**ultiple **A**ntenna **R**adio-interferometer for **B**aseline **L**ength **E**valuation (MARBLE)'.

2. Compact VLBI system

The compact VLBI system is the core equipment of the MARBLE system as explained in a previous section. To perform measurements at several calibration baseline in Japan, one of the important requirements of the VLBI system is transportability. We made two prototypes of transportable and

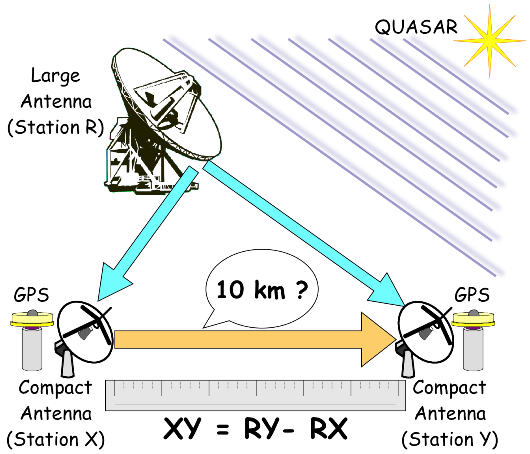

Figure 1. Measurement concept of the MARBLE (Multiple Antenna Radio interferometer for Baseline Length Evaluation).

compact VLBI systems from 2007 to 2009. This VLBI system consist of a small aperture antenna with drive unit of Az/El-mount type (figure 2), a receiver on ambient temperature, the K5 VLBI system [1][2], and a frequency standard etc. In the following, we describe details of the prototypes.

2.1 Small antenna and mount

The type of antenna is a front-fed paraboloid. The diameter of the reflectors are 1.65 m and 1.5 m for first and second prototype respectively. The two reflectors is the same F/D of 0.45. At focal point of the reflector, a wide-band feed (Quad-ridge horn antenna [3]) is placed. At the back of the feed, there is a front-end receiver with wide-band LNAs which can amplify up to 11 GHz. The front-end receiver also plays the roles of a polarizer and a frequency discriminator. At present, the receiver is only for S and X bands [4]. However, by replacing RF filters and other RF components, it will be able to receive the frequency bands from 2 to 11 GHz.

The antenna and mount can be divided into many parts without using a heavy machine. This feature is for transportability. So that we can easily compare the VLBI measurement with the GPS measurement, the antenna has the following features. The compact VLBI antenna can equip the GPS antenna on top of the El drive-unit, top of the Az drive-unit, and top of the base pillar. The antenna can also equip an target mirror for surveying at the azimuth-elevation crossing point which is reference point of the geodetic VLBI measurement.

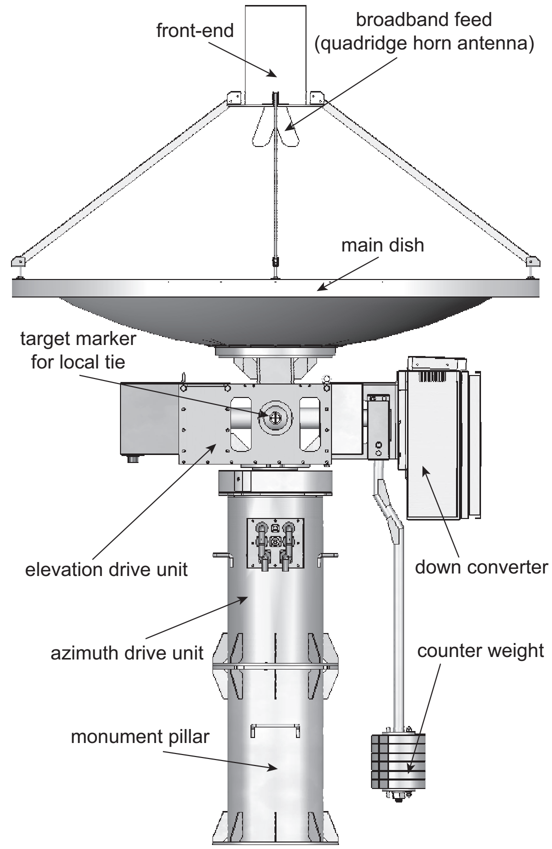

Figure 2. Schematic image of the antenna of the MARBLE system.

2.2 Frequency standards

The transportability is required for a frequency standard of the compact VLBI system as well as the antenna. However, a conventional hydrogen maser frequency standard is unsuitable to transportation.

The frequency standard that we are going to use is a laser-pumped Cs gas-cell frequency standard (hereafter, we call it 'Cs gas-cell oscillator') [5]. The size and weight of the oscillator is roughly equal to a desktop PC. The oscillator has a stability between the hydrogen maser frequency standard and the Cs beam type frequency standard. It is good enough to keep coherence for VLBI observation at the frequency of 8 GHz. Moreover, we confirmed the Cs-gas cell oscillator on geodetic VLBI using Koganei 11m antenna and Kashima 34 m antenna [6].

Another candidate of the frequency standard system is the radio frequency transfer using optical fiber [7]. The development purpose of this system is a comparison of optical frequency standards which have much higher frequency stability than that of conventional microwave frequency

Table 1. Results of experiments using the MARBLE system(s).

date	baseline	WRMS residual (psec)	baseline length*1 (mm)	formal error*1 u-d (mm)	e-w (mm)	n-s (mm)
2009. 6.25	R*2-B*3	58	193845.7 ± 2.4	6.2	2.7	3.5
2009.12.24	B*3-C*4	18	54184878.6 ± 2.7	19.5	2.7	2.6

*1 The errors represent 1 sigma of the formal errors.
*2 R : Kashima 11 m station
*3 B : first prototype of MARBLE
*4 C : second prototype of MARBLE

standards. Therefore, this system can transmit the radio frequency from the hydrogen maser oscillator without degradation of stability. The only disadvantage of the system is that it requires dark fibers.

2.3 It's applications

This compact and transportable VLBI system can be applied to various observations by the feature. For instance, it can be used for the VLBI time and frequency comparison [8]. Only one VLBI station with a large antenna is needed for this purpose. By bringing a compact VLBI station with small antenna, time and frequency comparison is possible anywhere.

In VLBI2010 project, it is expected that the compact VLBI station with small antenna can be used for gravity and thermal deformation model construction of a large VLBI antenna [9]. By repeating geodetic VLBI measurement using a large antenna and a small stable antenna placed near the large antenna, we will be able to find a signal of deformation of the large antenna.

3. Performance tests of the prototypes

To test the performance of those prototypes, we installed the first prototype near the Kashima 34 m antenna in NICT in December, 2008, and installed the second prototype near the Tsukuba VLBI station (32 m antenna) in GSI in October, 2009. Before setting up the second prototype, we performed general geodetic VLBI experiment of 24 hours using the first prototype. In the experiment, we also used the Tsukuba VLBI station and the Kashima 11 m station. The hydrogen maser oscillators were used as frequency standards in each station, observed band was S and X band, the total recording data rate was 512 Mbps in the experiment. As a result of the experiment, we successfully obtained fringes over the 24 hours, and could estimate baseline length between the Kashima 11 m station and the first prototype about 200 m (table 1). The formal error of the measured baseline length was 2.4 mm.

After installation of the second prototype, we carried out geodetic VLBI experiment of 24 hours using the two prototypes and the Tsukuba VLBI station. The frequency standards, observed band and the total recording rate were same as former experiment. We could estimate baseline length between the two prototypes about 54 km (table 1). The formal error of the estimated baseline length was 2.7 mm. However, in this experiment, there were many outliers of several tens nsec in delay residuals. We don't find the origin of the failure ,though we expect that the cause is the failure of bandwidth synthesis, so far. Especially, since the influence was large in S band, we did not include the time delays from S band in the analysis. Though there was such a problem, the baseline length was able to be measured by using the two prototypes. This result is evidence that these prototypes is usable for geodetic VLBI. Moreover, there is room for making the observation data rate higher. The higher observation data rate will bring a smaller measurement error of a baseline length.

4. Conclusion and outlook

We made the two prototypes of compact and transportable VLBI system. We performed geodetic VLBI experiments using these prototypes. The formal errors of the baseline length estimation are about 2 to 3 mm. From the result, we confirm that these prototypes can be used on geodetic VLBI. There is room for improvement of the error of the measurement. If we identify the cause, and it is possible to solve it, the measurement error will be decreased. On the other hand, higher speed A/D sampler (ADS3000+) available [10]. The measurement error will be decreased by using ADS3000+ also. To obtain a higher measurement precision than the current precision, we proceed the development. We have a plan to make another prototype. We will review the antenna design and the receiver design, and we will make more a sensitive VLBI station.

This compact and transportable VLBI system can be applied to various observations. We are also planning to apply our prototype into the time and frequency comparison experiment in this year.

Acknowledgments: We wish to express our gratitude to Teruaki Orikasa, Yoshiyuki Fujino, Jun Amagai, Mamoru Sekido, Eiji Kawai, Moritaka Kimura and Junichi Nakajima of NICT by a lot of advices for this research. We are very grateful for cooperation in the experiments by Hiromitsu Kuboki, Masanori Tsutsumi and Shingo Hasegawa of NICT. The part of this work was supported by a Grant-in-Aid for scientific research (KAKENHI, No.212410043). We used CALC/SOLVE made by GSFC for VLBI analysis.

References

[1] Koyama,Y., T.Kondo, H.Osaki, A.Whitney, and K.Dudevoir, Rapid turnaround EOP measurements by VLBI over the Internet, Proceedings of the IAGG02 Symposium in the23rd IUGG General Assembly, Sapporo Japan, July, 2003.

[2] Kondo,T., Y. Koyama, R.Ichikawa, M.Sekido, E.Kawai, and M.Kimura, Development of the K5/VSSP System, J. Geod, Soc. Japan, Vol.54, No 4, pp. 233-248, 2008.

[3] Rodriguez,Vincent., A Multi-octave Open-boundary Quad-ridge Horn Antenna for Use in the S- to Ku-band, Microwave Journal, 49, 84-92, 2006.

[4] Ichikawa,R., A.Ishii, T.Takiguchi, Y.Koyama, T.Kondo, K.Kokado, S.Kurihara, and S.Matsuzaka, Present Status and Outlook of Compact VLBI System Development for Providing over 10 km Baseline Calibration, IVS TDC-News, No. 30, pp. 22-25, 2009.

[5] Ohuchi,Y.,H.Suga, M.Fujita, T.Suzuki, M.Uchino, K.Takahei, M.Tsuda, and Y.Saburi, A HIGH-STABILITY LASER-PUMPED Cs GAS-CELL FREQUENCY STANDARD, Proc. IEEE/EIA International Frequency Control Symp., pp.651-655, 2000.

[6] Ishii,A., R.Ichikawa, H.Takiguchi,H.Kuboki, M.Sekido, Y.Koyama, and Y.Ohuchi, Evaluation of a Laser-pumped Cs Gas-cell Frequency Standard on Geodetic VLBI,Journal of the Geodetic Society of Japan, Vol. 54, No. 4, pp.259-268, 2008.

[7] Kumagai,M., M.Fujieda, S.Nagano, and M.Hosokawa, Stable radio frequency transfer in 114 km urban optical fiber link, OPTICS LETTERS, Vol. 34, No. 19, October 1, 2009.

[8] Takiguchi,H., Y.Koyama, R.Ichikawa, T.Gotoh, A.Ishii, and T.Hobiger, Comparison Study of VLBI and GPS Carrier Phase Frequency Transfer -Part- Ⅱ, IVS TDC-News, No. 30, pp. 26-29, 2009.

[9] Petrachenko,1B(chair), A.Niell, D.Behrend, B.Corey, J.Bohm, P.Charlot, A.Collioud, J.Gipson, R.Haas, T.Hobiger, Y.Koyama, D.MacMillan, Z.Malkin, T.Nilsson, A.Pany, G.Tuccari, A.Whitney, J.Wresnik, Design Aspects of the VLBI2010 System Progress Report of the IVS VLBI2010 Committee, NASA/TM-2009-214180, June, 2009.

[10] Takefuji,K., Y.Koyama, and H.Takeuchi, First Fringe Detection with Next-Generation A/D Sampler ADS3000+, IVS TDC-News, No. 30, pp. 17-21, 2009.

Current Status of Next Generation A/D Sampler ADS3000+

Kazuhiro Takefuji (*takefuji@nict.go.jp*)[1], **Masanori Tsutsumi**[1], **Hiroshi Takeuchi**[2], **and Yasuhiro Koyama**[1]

[1] *Kashima Space Research Center, National Institute of Information and Communications Technology, 893-1 Hirai, Kashima, Ibaraki 314-8501, Japan*
[2] *Institute of Space and Astronautical Science (ISAS), Japan Aerospace Exploration Agency (JAXA) 3-1-1 Yoshinodai, Sagamihara, Kanagawa 229-8510, Japan*

Abstract: A high-speed A/D sampler, we called the ADS3000+, has been developed in 2008, which can sample one analog signal up to 4Gbps to versatile Linux PC (K5/VSI). After A/D conversion, the ADS3000+ is possible to realize digital signal processing such as real-time DBBC (Digital Base Band Conversion) and realtime simple CW RFI filtering with equipped FPGAs. In June 2010, DBBC first fringe is obtained between Kashima 11m antenna and Koganei 11m antenna. The ADS3000+ will not only be used for VLBI, but also other versatile science purposes.

1. Introduction

National Institute of Information and Communications Technology (NICT) has been developing VLBI observation systems and data processing systems since 70s. The K5 VLBI system is designed with the commodity products such as personal computers, hard disks, and network components. This strategy has been quite successful to develop highly flexible and high performance observation systems and data processing systems for VLBI. K5/VSI series are realized by high speed AD sampler units and a commodity Linux PC system to record data with the VSI-H (VLBI Standard Interface - Hardware specifications). VSI-H was proposed to define standard interface for the high speed data transfer between data input modules, data transfer modules, and data output modules to improve the compatibility between next generation VLBI observing systems and the correlator systems. Three high speed AD sampler units, ADS1000, ADS2000, and ADS3000, have been already developed to support various sampling modes. ADS1000 can sample one baseband channel at the sampling rate of 1024Msps/2bit. ADS2000 can sample 16 baseband channels at the sampling rate of 64Msps suitable for geodetic VLBI observations with the bandwidth synthesis method. ADS3000 can sample wide range of baseband frequency band up to 1024MHz with the sampling rate of 2048Msps[2]. Currently, ADS3000+(Figure.1) has been developed to support 4Gbps*1ch and 2Gbps*2ch, 1Gsps*4ch sampling modes by using faster AD sampler chip[1]. ADS3000 and ADS3000+ are equipped with FPGA chips to realize digital baseband converter (DBBC) with user-selectable bandwidth of 4 - 32 MHz. We will present more detail about the newly designed ADS3000+ system in this article.

Figure 1. ADS3000+ appearance. Front display shows clock status, IP setting, input bit histogram and many other imformations

Size	EIA 2U (480mm x 88mm x 430mm)
Reference	10MHz 0dBm+-3dBm, 1PPS (50ohm)
IF input	+-250m Vp-p (50ohm)
Output	VSI-H compliance
Control	RS232-C (D-sub 9pin male),100Base-Tx
Power supply	AC100-240V
A/D chip	e2V EV8AQ160
FPGA chip 1	Xilinx Virtex5 XC5VLX110
FPGA chip 2	Xilinx Virtex5 XC5VLX220
Sampling Modes	4096Msps x 1ch
	2048Msps x 2ch
	1024Msps x 4ch (DBBC mode)

Table 1. Specifications of the ADS3000+ unit. FPGA chip is possible to replace larger size one (ex XC5VLX330)

2. A next-generation A/D sampler ADS3000+

The ADS3000+[1] is newly-extend A/D sampler from the ADS3000 system by adopting supporting various sampling mode. faster A/D sampler chip and two new FPGA chips replacing one FPGA

[1]More information and news is available at http://www2.nict.go.jp/w/w114/stsi/K5/

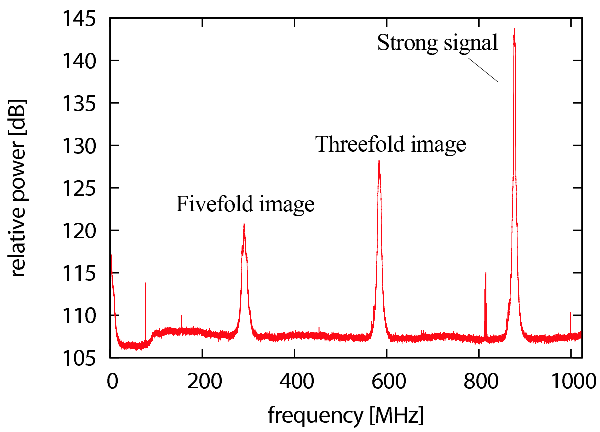

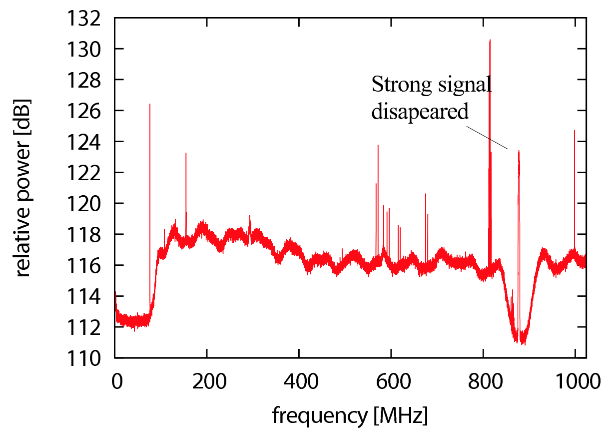

Figure 2. Left: With omni-directional antenna and wide-band receiver 100-1024MHz and detected actual radio condition around Kashima space research center. At 880MHz, strong signal from handy base station can be seen. The base station signal is too strong to obtain proper dynamic range. Right: After adopted BEF, strong base station nt only becomes weak, but also it could be measured another radio signals with improved dynamic range.

chip. It has a capability to sample analog data up to 5GHz at the highest speed. However one VSI-H (VLBI Standard Interface) interface is connected with PC limited up to 2Gbps (Giga bit per second), the maximum sampling speed via two VSI-H connection becomes 4Gbps ADS3000+ has four VSI-H output port, 8Gbps record is theoretically possible for connecting four VSI-H PC at maximum.

The ADS3000+ digitizes analog signal 1Gsps * 4ch, 2Gsps * 2ch, 1Gsps * 4ch. Moreover, various signal processing such as DBBC (Digital Base-Band Converter) can be performed with FPGA chips inside the ADS3000+. Table.1 shows the major specifications of the ADS3000+ system. Standard sampling modes up to 4GHz has been evaluated. and 4GHz sampling fringes was obtained in 2009[3].

3. Realtime FIR filtering, RFF mode

With FPGA technique, real-time FIR filtering signal processing, called RFF mode is realized in 2Gsps * 2ch mode at maximum. We actually adopted the RFF mode to radio signals round Kashima Space Center. This is shown in Figure.2. In this case, we designed Band elimination filter(BEF) for suppressing strong signal. In RFF mode, filter coefficient is limited 65taps 8bit range. However, any filter can be designed in these conditions. The RFF is also used for VLBI purpose. For example, real-time Hibert transform which make 90 degree shift like 90 degree hybrid is possible. As for liner polarization to cirular polarization conversion, it would be possible to apply following RFF. One channel of RFF is put Hilbert transform coefficient, and another channel is put meaningless coefficient only for synchronizing delay.

Sample speed	Quantize	VSI clock
8Msps*16ch	4bit	Fix: 64MHz, Variable 8MHz
16Msps*16ch	4bit	Fix: 64MHz, Variable 16MHz
32Msps*16ch	4bit	Fix: 64MHz, Variable 32MHz
64Msps*16ch	4bit	Fix: 64MHz, Variable 64MHz
1024Msps*4ch	1bit,2bit	Fix: 64MHz

*Table 2. Specification of ADS3000+ DBBC mode. One VSI-H of DBBC generates is 16ch * 2bit, 8ch * 4bit and VSI clock speed is able to chose fix type or variable. 1024Msps * 4ch is supported in DBBC.*

4. DBBC on the ADS3000+

DSP in ADS3000+ is realized DBBC. There are 16ch DBBCs inside ADS3000+. Specification of DBBC is shown in Table.2. 16ch DBBCs*2bit or 8ch DBBCs*4bit can be selectable. Output of DBBC occupies two VSI port. When 16ch DBBCs*2bit is used, upper 2bit is for VSI-1 and lower 2bit if for VSI-2. and when 8ch DBBCs*4bit is used, upper 8ch is for VSI-1, and lower 8ch is for VSI-2. Figure.3 shows DBBC inside flow chart. First digital data comes from A/D, they are multiplied by NCO (numerical controlled oscillator) which is possible to tune frequency by 1Hz resolution and angular acceleration. After frequency shifted, next comes filtered CIC and FIR. CIC (Cascade Integrator Comb)is not only small circuit but also useful LPF. Finally complex or real (USB or LSB) signal is generated. A delay between 16ch DBBCs is calibrated to zero in all mode. User dose not need to care about de-

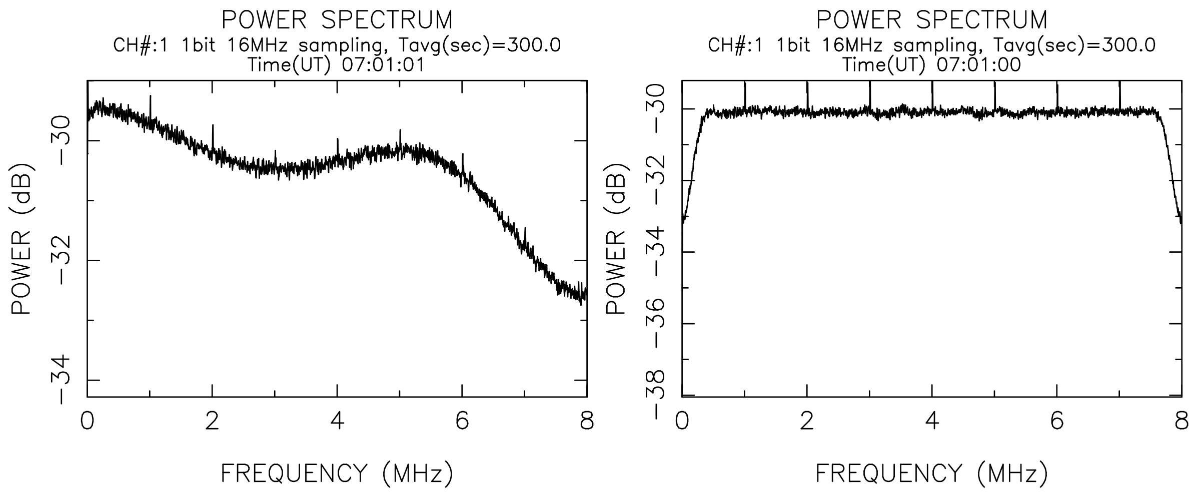

Figure 4. X-band spectra of K5/VSSP32 sampler(Left) and DBBC of ADS3000+ (right) output. Downside spectrum of K5/VSSP32 is caused by an effect of image-rejection mixer. Meanwhile spectrum of DBBC shows line symmetry and flat shape, so this flat band-character will be increased SNR better than K5/VSSP32 system.

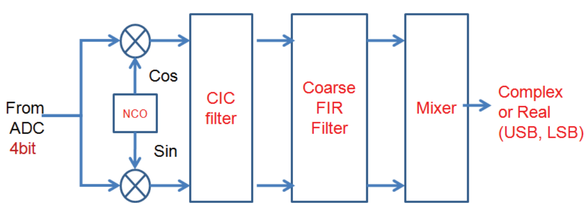

Figure 3. DBBC flow in ADS3000+. The DBBC is modified Weaver method which is multiplicated by NCO and filtered out. To suit FPGA capacity CIC filter (Cascade Integrator Comb) is applied. There are 16 DBBCs in ADS3000+. Each DBBC can generate Complex or Real (USB or LSB) with 4,8,16,32 MHz bandwidth

lay inside DBBCs. Now we perform final check of DBBC. Figure.4 shows X-band IF spectra of K5/VSSP32 and DBBC. The K5/VSSP32 digitizes analog signal whose frequency is converted by image-rejection mixer. Due to characteristic of image-rejection mixer, band-character by K5/VSSP32 sampler is downside shape. Meanwhile band-character by DBBC shows line symmetry. Lower and upper edge of the band-character is filtered out. It is difficult to use 10kHz phase calibration signal for geodetic VLBI purpose. However, flat-shaped band-character by DBBC will increase SNR of fringe. Figure.5 shows zero-baseline test between K5/VSSP32 and DBBC. The correlation coefficient is not 1 but about 0.5. It may cause by difference between downside band-character and flat-shape band-character. Figure.6 shows first detected fringe between K5/VSSP32 in Koganei 11m antenna and DBBC in Kashima 11m antenna whose baseline is about 140km in June 2010.

5. Summery

We successfully detect first fringe between DBBC(ADS3000+) - K5/VSSP32 system in this June 2010. Next we will set ADS3000+ in both stations and detect DBBC-DBBC fringe. And We could suppress stronge RFI signal with RFF mode. With installed real-time filtering DSP and DBBC DSP, ADS3000+ becomes more powerful tools for not only VLBI and but astronomy and science.

Developments of the ADS3000+ system cooperative efforts between NICT, JAXA/ISAS, and COSMO RESEARCH Corp[2]. The authors would like to thank for cooperation of the Kashima VLBI team.

References

[1] Koyama, Y., T. Kondo, M. Sekido, and M. Kimura, Developments of K5/VSI System for Geodetic VLBI Observations TDC News, IVS NICT-TDC News, **No.29**, pp.15-18, 2008.

[2] Takeuchi, H., M. Kimura, J. Nakajima, T. Kondo, Y. Koyama, R. Ichikawa, M. Sekido, and E. Kawai, Development of 4-Gbps Multi-functional VLBI Data Acquisition System, Publications of the Astronomical Society of the Pacific, **Vol.118**, pp.1739-1748, 2006.

[2] http://www.cosmoresearch.co.jp

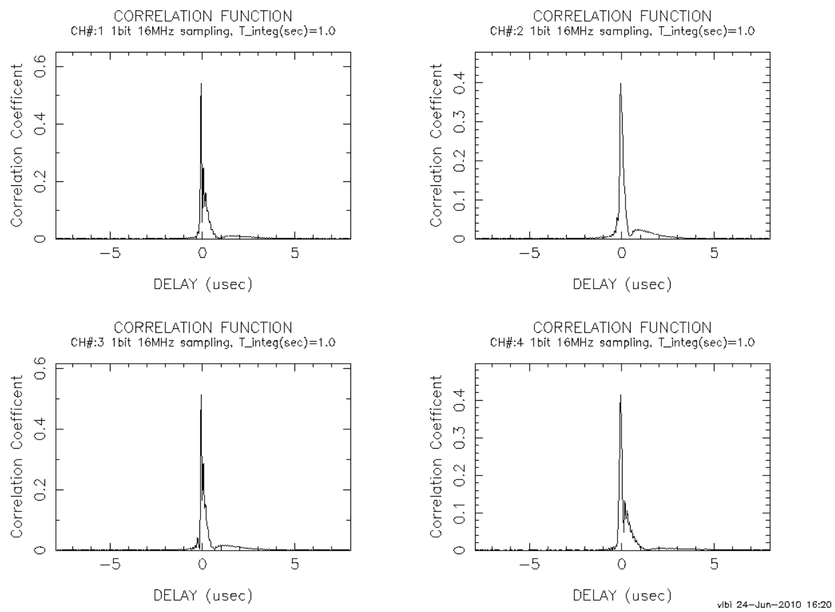

Figure 5. Cross-correlation between K5/VSSP32 and DBBC. By difference of these spectra, correlation coefficient is lower than 1.

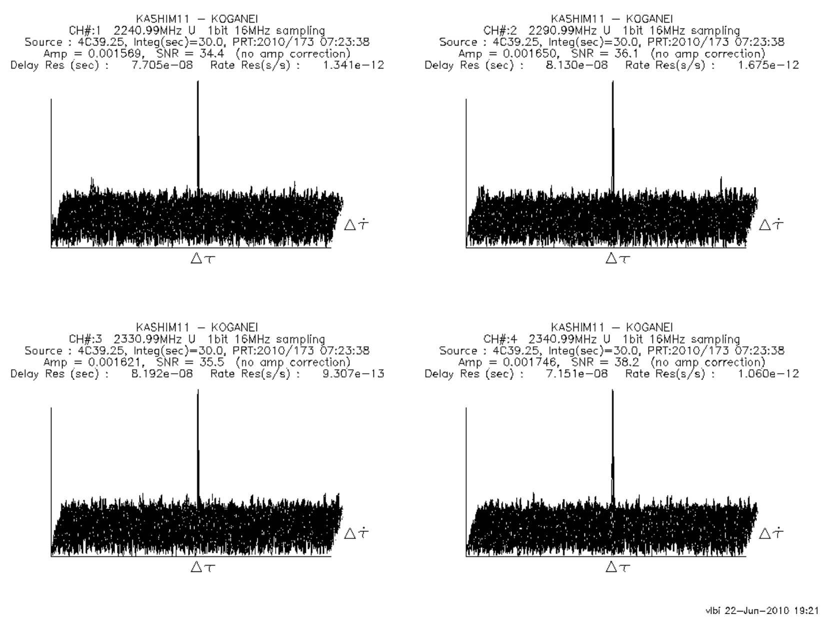

Figure 6. First detected fringe between Kashima 11m antenna (DBBC) and Koganei 11m antenna (K5/VSSP32)

[3] Takefuji, K., H. Takeuchi, and Koyama, Y., First Fringe Detection with Next-Generation A/D Sampler ADS3000+ TDC News, IVS NICT-TDC News, **No.30**, pp.17-21, 2009.

GPU based GNSS software receivers - status quo and plans

Thomas Hobiger (*hobiger@nict.go.jp*), **Tadahiro Gotoh, Jun Amagai, Tetsuro Kondo and Yasuhiro Koyama**

National Institute of Information and Communications Technology
4-2-1 Nukui-Kitamachi, Koganei
184-8795 Tokyo
Japan

Abstract: Software receivers for GNSS are a flexible and cheap alternative to hardware solutions, and the usage of graphics processing units (GPUs) allows to operate the receiver even in real-time (Hobiger et al., 2010 [1]). Recent developments with this receicer technology are summarized and plans for new applications are stated in this report.

1. Introduction

Off-the-shelf graphics processing units provide low-cost massive parallel computing performance, which can be utilized for the implementation of a GNSS software receiver. In order to realize a real-time capable system the crucial stages of the receiver should be optimized to suit the requirements of a parallel processor. Moreover, the receiver should be capable to provide wider correlation functions and provide easy access to the spectral domain of the signals. Hobiger et al. (2010) demonstrated that such a GNSS software radio can be realized with minimal cost enabling all the feature mentioned above.

2. New features

Over the last nine months many parts of the software receiver were re-designed and new features were added in order to allow for more reliable signal detection. Moreover, as graphic card vendors improved their drivers and libraries, applications ran faster and programming and debugging became more straightforward. The major improvements are listed in the following sub-sections.

2.1 Software re-design

The complete host code, which was originally designed in C-language, has been re-written in C++ in order to extend the flexibility. Thereby the device programs which are written in CUDA, are binded via shared objects and the usage of C++ enables to link to external libraries like BOOST which is used for time-tagging within the receicer. Moreover, NetCDF libraries are used to output results to binary files with sampling rates of up to 1000 Hz, without decreasing the performance of the receicer. Additionally, detection and usage of multi-GPU environmets is implemented as well as new GNSS signal are now supported. The orbit module of the receiver has been revised as well, allowing now to use broadcast orbits from the Internatial GNSS Service (IGS) or to utilize the decoded information from the receipt navigation message streams.

2.2 Open-look tracking

As one of the new receiver features an option for open-loop tracking has been implemented. Other than in the closed-loop mode, where delays and phases (respectively Doppler shifts) are updated via the correlator output, it is possible to run the software receiver exclusively without such a feedback (see figure 1). Thereby orbit information pro-

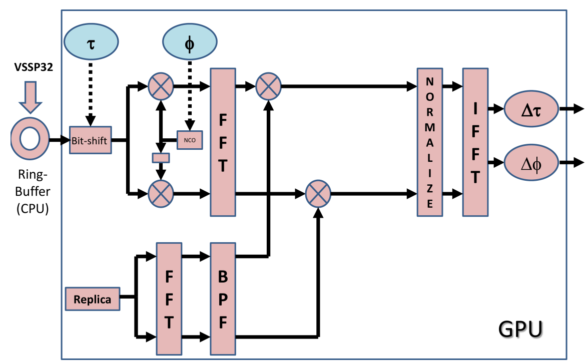

Figure 1. The software receiver in open-loop tracking. Instead of updating the read pointers and the numerical controlled oscillator with delays and phases from prior receiver output, one can use external a-priori information to track GNSS signals.

vided from the IGS can be used to compute delay and phase values which drive the receiver. As broadcast ephemeris might not be good enough for highly precise applications, also SP3 orbit information can be input and used for such purposes. Open-loop tracking allows to monitor very weak signals at low elevations, which enables the receiver to be used for studies of the atmosphere and ionosphere. Although the open-loop technique is mainly deployed in GNSS occultation satellites, such a receiver mode can also be useful for ground based stations which are not restricted in their field-of-view at lower elevations. Given that the receiver is placed on a high enough location (e.g. a mountain) and that the antenna allows tracking of signals below the local horizon, one can use this technique to probe the atmosphere horizontally and even at negative elevation angles.

2.3 Coherent integration

In the case that the signal-to-noise ratio (SNR) of the incoming signals is sufficiently high, the receiver will compute the cross-correlation function for a given short time-span, which e.g. in the case of the L1 C/A code can be chosen down to 1 millisecond. If the SNR gets lower, wrong detections of the correlation peak become more often and the receiver will start to loose lock. Other than open-loop tracking, which has been discussed before, one can integrate results coherently over several periods in order to surpress the noise-like components which can lead to wrong detections. Figure 2 depicts how such an integrator can be included in the software receiver processing chain.

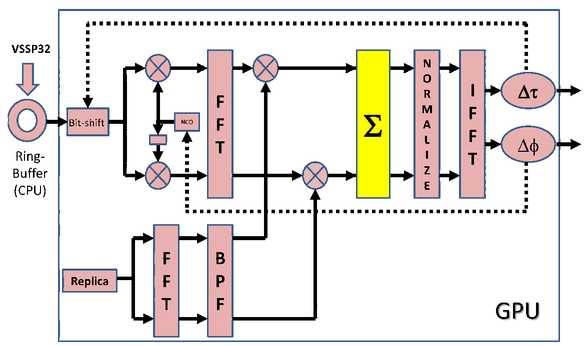

Figure 2. The software receiver with a coherent integration stage (yellow).

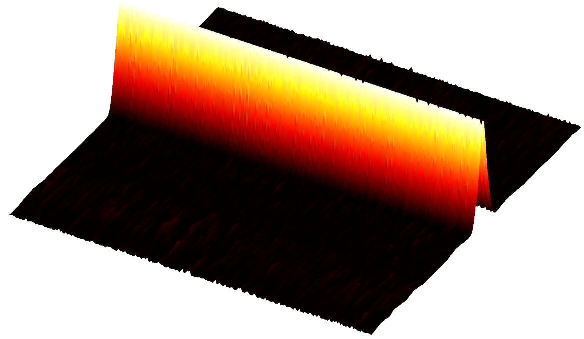

Figure 3. Cross-corrlation function of PR10 (66.3 degree elevation) from Mar.25, 2009 4:17:07, showing the first 256 ms of data and the inner 128 lags of the 8192 FFT points.

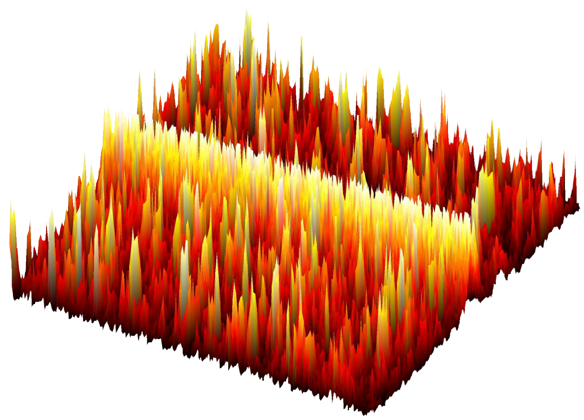

Figure 4. Cross-corrlation function of PR04 (12.1 degree elevation) from Mar.25, 2009 4:17:07, showing the first 256 ms of data and the inner 128 lags of the 8192 FFT points.

2.4 A test with coherent integration

In order to demonstrate the effectiveness of coherent integration data taken with a sampling rate of 8 Msps on March 25th, 2009 was fed to the software correlator and processed with and without coherent integration. Figure 3 shows the cross-correlations functions for a PRN with high SNR and figure 4 displays the results from processing of a weak signal. Coherent integration of 4 code-lengths (i.e. 4 ms) already helps to improve the detection of the correct correlation peak (figure 5) and integration over 8 ms (figure 5) already removes any wrong detection during the processing of the 256 ms datablock. Applying the three strategies (no integration, 4 ms and 8 ms integration) for PRN 04 to the first 5 seconds after 4:17:07 allows to compare the performance of the different approaches. The weigthed-RMS (WRMS) without coherent integration equals to 410 ns, which makes clear that at many epochs a wrong peak is picked up by the receiver. This measure improves to 209 ns when applying the 4 ms integration scheme, which still has some wrong detections. The 8 ms integration results, which are free of outliers provide an WRMS of 8 ns which is within the expected range of the C/A code precision.

2.5 Speed-up due to coherent integration

The coherent integration does not only improve the quality of the software receiver, but also helps to speed-up the processing, pushing it towards real-time capability. As shown in figure 2, the parts after the the summation are only called every N periods. Thus, assuming that the cost of the inverse FFT are equal to those of the FFT once can state that with coherent integration of N summations, $(N-1)$ FFT operations can be saved. Moreover the

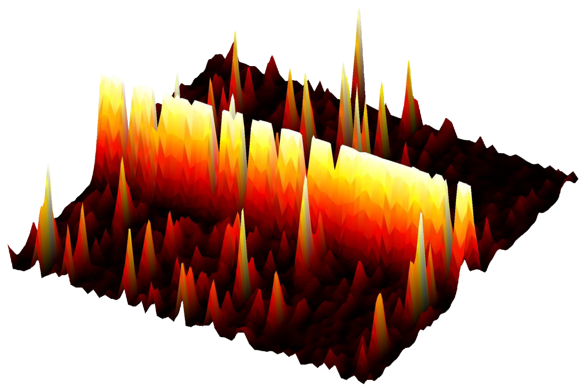

Figure 5. Cross-corrlation function of PR04 (see figure 4) after 4 ms coherent integration.

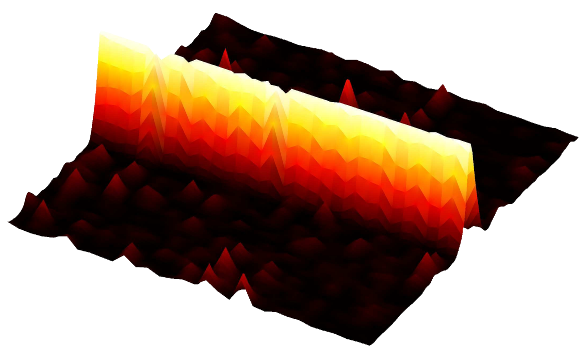

Figure 6. Cross-corrlation function of PR04 (see figure 4) after 8 ms coherent integration.

quite large cost of normalizing the cross-correlation function as well as the peak search will be reduced as well. For shorter FFT-sizes, i.e. lower sampling rates, FFTs are much cheaper than normalizing and peak search, which will lead to significant speed-ups. For higher sampling rates, which require larger FFT sizes, the compution of the FFTs will take most of the time, which leads to an estimated saving of approximately $(N-1)/(2N) \approx 50\%$. Figure 7 confirms the asumptions for lower data-rates and the speed-up of roughly 50 % can be seen in processing results with 32 Msps (figure 8).

3. GNSS-Reflections

Beside the classical GNSS derived products, it can be also used as a remote sensing tool. Signals which reach the ground and are reflected before arriving at the antenna change from right-hand to left-hand polarization. Thus, if two atennas, one up-looking (RCHP) and one down-looking (LHCP) are deployed at the same site one can cross-correlate the two signals. Thereby the cross-

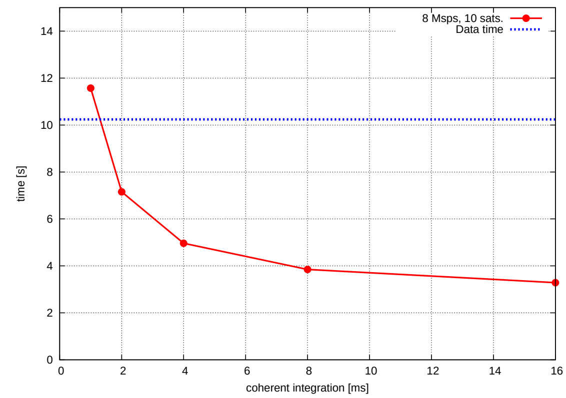

Figure 7. Speed-up for different integration lengths w.r.t. a receiver without coherent integration (1 ms). The test-data set was recorded with 8 Msps, whereas 10 satellites were visible at that time. The blue dashed line shows the real-time criteria.

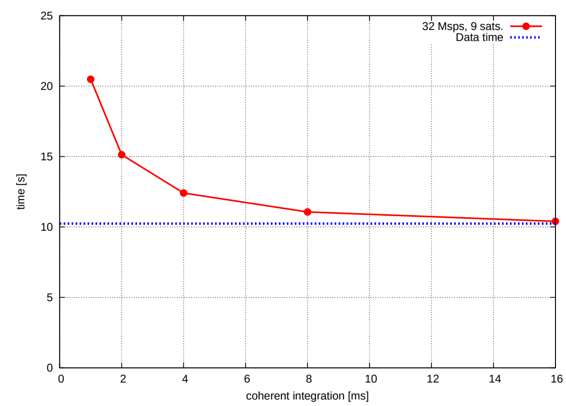

Figure 8. Speed-up for different integration lengths w.r.t. a receiver without coherent integration (1 ms). The test-data set was recorded with 32 Msps, whereas 9 satellites were visible at that time. The blue dashed line shows the real-time criteria.

correlation function

$$\int_{-\infty}^{\infty} S_{RHCP}(\tau)S_{LHCP}(\tau+t) = F(\Delta H, el, \sigma_{surf}, \dots) \tag{1}$$

is depending on the geometry w.r.t. the concerning satellite (as a function of the receiver height and the elevation angles). Moreover, the pattern of the cross-correlation function and its amplitude allow to deduce the physical properties of the scattering surface. Based on the experience gained from the development of the software receiver we will start to implement a GPU based processing scheme for GNSS-R and test it with real-data.

4. Outlook

New GPU technology available since April 2010 is expected to boost the performance of the developed receiver and push the real-time ability towards higher sampling rates. On the other hand, new signals like L2C require more complex processing stages which need careful design for utmost high data-throughput. Once all components of a dual-frequency software reveiver are implemented, it will be tested in a 24h real-time environment and its results will be compared against those of a commercial hardware receiver. In order to reduce the total cost of the system, other RF front-end solutions will be tested as well.

Acknowledgments: Parts of this work were supported by a Grant-in-Aid for Scientific Research (KAKENHI-21241043).

References

[1] Hobiger T., T. Gotoh, J. Amagai, Y. Koyama, T. Kondo (2010), A GPU based real-time GPS software receiver, GPS Solutions, 14, 2, 207–216, 2010.

Automated processing of VLBI experiments with c5++

Thomas Hobiger[1] (*hobiger@nict.go.jp*), **Tadahiro Gotoh**[1], **Toshimichi Otsubo**[2,1], **Toshihiro Kubooka**[1], **Mamoru Sekido**[1], **Hiroshi Takiguchi**[1] and **Hiroshi Takeuchi**[3]

[1] *National Institute of Information and Communications Technology*
4-2-1 Nukui-Kitamachi, Koganei
184-8795 Tokyo
Japan

[2] *Hitotsubashi University*
2-1 Naka, Kunitachi
186-8601 Tokyo
Japan

[3] *Japan Aerospace Exploration Agency, Institute of Space and Astronautical Science (ISAS)*
3-1-1 Yoshinodai, Sagamihara, Kanagawa
229-8510, Tokyo
Japan

Abstract: Processing of space geodetic techniques should be carried out with consistent and utmost up-to-date physical models. Therefore, c5++ is being developed, which will act as a framework under which dedicated space geodetic applications can be created. Due to its nature, combination of different techniques as well as automated processing of VLBI experiments will become possible with c5++.

1. Introduction

An analysis software package based on Java and named CONCERTO4 (Otsubo and Gotoh, 2002 [3]) enabled the user to consistently process SLR, GPS and other satellite tracking data. The next version of this program package will also include VLBI as additional space-geodetic technique. As the software is currently being redesigned and completely re-written in C++, the requirements for VLBI data analysis could be taken into account. Moreover, combination of space geodetic techniques was considered during the design phase.

2. Space geodesy with c5++

Basically, c5++ provides the framework (figure 1) under which space geodetic applications can be built. Thus, stand-alone technique specific applications can be developed or multi-technique solutions can be realized.

Thereby consistent geophysical and geodetic models, based on the IERS conventions 2003, are applied to each technique, which enables the combination either on the observation level or on the normal-equation level. External libraries, which are available as open source packages, are utilized for data input/output as well as vector and matrix operations. c5++ has been successfully compiled and tested under Windows, Linux and Mac OS using 32-bit and 64-bit environments. Modules are commented within the code and information is extracted via Doxygen, which outputs on-line the documentation (in HTML) and/or an off-line reference manual.

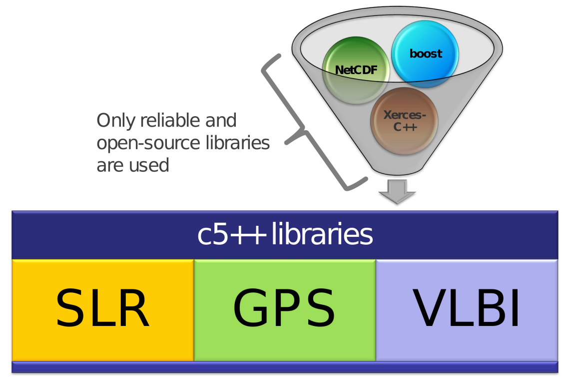

Figure 1. Building space geodetic analysis software for SLR, GPS or VLBI by interfacing the c5++ libraries.

2.1 Libraries resp. classes contained within c5++

Table 1 lists the most relevant classes together with their functionality. Space-geodetic software can be build, by interfacing the required modules as well as other applications can be realized from this framework.

2.2 VLBI with c5++

Based on the main classes of c5++ a dedicated VLBI analysis chain can be implemented with minimal efforts. Thereby, modules can be attached like building blocks and even dedicated/specialized VLBI software solutions can be realized, without in-depth knowledge of the specific classes. In order to fulfill the requirements of different applications the following observation formats are supported within c5++

- NGS
- NetCDF
- MK3
- Raw correlator (K5 format)

Name	Functionality
C5Time	Implements internal time container, allows input of UTC, TAI, TT, MJD, JD and converts between the time systems using an internal storage format.
C5Math	Main math library, which provides dedicated matrix operations and geodetic tools.
Transform	Transforms positions between TRF and CRF
Ephm	Reads JPL binary ephemeris and provides position/velocity of any given celestial body in a user-defined frame
Displacement	Computes solid Earth tides, ocean and atmosphere loading corrections
Accel	Provides various accelerations respectively forces which act on a satellite
Cowel	Fast and accurate orbit integrator
Param	Is the backbone of c5++ which manages all kind of selectable parameters and carries out automatic interpolation for time-dependent parameters.
ParamIO	Reads and writes parameters/results in XML format
Relativity	Computes relativistic corrections for GPS and SLR and transforms VLBI delays into the TCG frame
C5ObsData	Reads observational data and stores it in a STL container class.
Antenna	Antenna/telescope specific corrections models (deformations, axis offsets, ...)

Table 1. c5++ libraries and their functionality.

In the first stage all modules are designed to work properly and give correct results. Optimization concerning the improvement of processing speed will be made, once testing and verification has been completed.

3. Multi-technique combination

Since all space-geodetic techniques can utilize the same physical and geophysical models from c5++, consistent combination across the techniques can be realized. Thereby, results can be either combined on the normal-equation level or on the observation level, in accordance with the goals of the Global Geodetic Observing System (GGOS). Moreover, novel applications like spacecraft tracking can be developed, whereas orbit calculations based on multi-technique observations (GNSS, SLR and VLBI) are expected to provide an utmost accurate 3D trajectory of the satellite.

4. Automated UT1 processing

Beside multi-baseline sessions, regular single baseline VLBI experiments are scheduled in order to provide estimates of UT1 for the international space community. As shown by Sekido et al. (2008) [4] and Matsuzaka et al. (2008) [2] the latency of these Intensive experiments could be improved tremendously and results could be made available within less than an hour if e-VLBI and automated processing routines were applied. If the whole processing pipeline works well, results can be obtained even within minutes after the last scan has been recorded, which is highly appreciated by the users community as discussed in Luzum and Nothnagel (2010) [1]. Based on the experience gained over the last two years, the automated processing chain will be improved and the analysis software used until know will be replaced by c5++. Since the correlator output format can be read directly with c5++, no intermediate interface is necessary. Moreover, ambiguity resolution and ionosphere correction can be done within the framework of c5++. Not only the target parameter, i.e. UT1, will be estimated with c5++ but also databases for the VLBI community are expected to be created with that software. As shown in figure 3, it will be also possible to input a-priori delay models to the correlator in order to achieve highest possible consistency between all the data processing stages. First tests with c5++ will be carried out in the middle of 2010 and as soon as the whole processing pipeline is operating stable enough, results will be submitted to IERS in order to be included for UT1 predictions. Thus, a focus will be set on robust and reliable automated ambiguity resolution, in order to allow for completely unattended operation. Additional functions will include automated reporting of re-

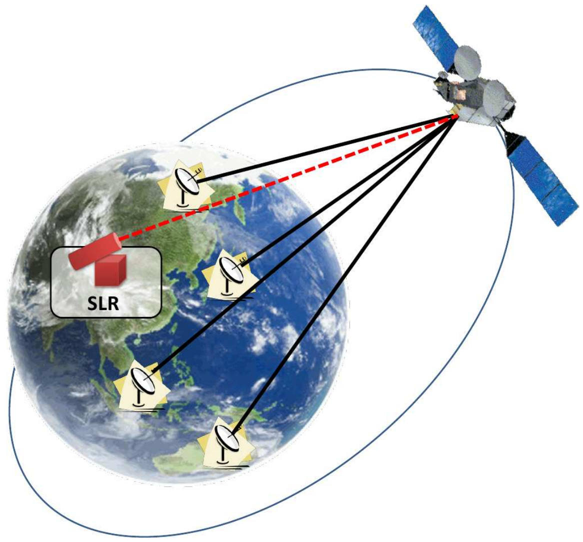

Figure 2. Since c5++ is also designed for satellite techniques, existing modules and models can also be utilized to do space-craft tracking either by VLBI or by a combination of several techniques. E.g. an integration of SLR and VLBI tracking will allow a computation of highly accurate orbit arcs

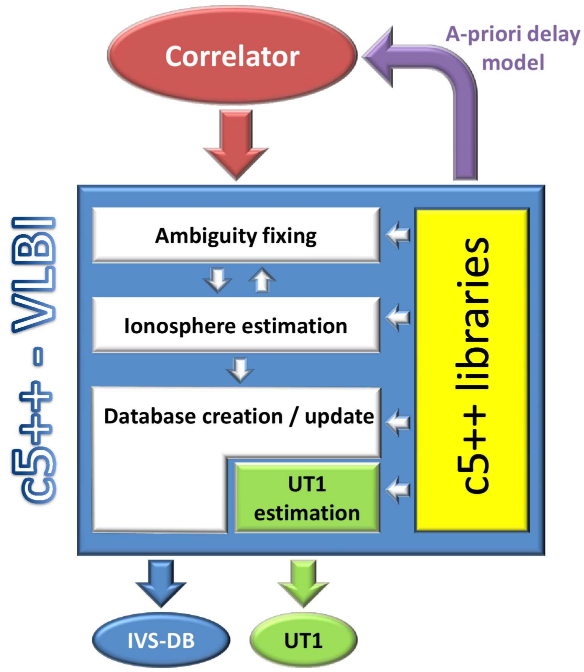

Figure 3. Flow-chart of automated VLBI analysis and UT1 estimation.

sults to international services as well as export of standard formats for independent analysis within the space-geodetic community. Once the UT1 processing scheme has been established and has been gone operational, the software will be extended to derive all three Earth orientation parameters from multi-baseline experiments. This will require also modifications of the ambiguity resolution strategy which gets slightly more complex as compared to single-baseline experiments.

Acknowledgments: Parts of this work were supported by a Grant-in-Aid for scientific research (KAKENHI, No. 24241043) from the Japan Society for the Promotion of Science (JSPS). We highly appreciate the support from the VieVS group at Vienna University for helping us with the validation of our modules.

References

[1] Luzum B. and A. Nothnagel, Improved UT1 predictions through low-latency VLBI observations", Journal of Geodesy, in print, 2010.

[2] Matsuzaka .S, H. Shigematsu, S. Kurihara, M. Machida, K. Kokado and D. Tanimoto, Ultra Rapid UT1 Experiments with e-VLBI, Proceedings of the 5th IVS General Meeting, 68–71, 2008.

[3] Otsubo T. and T. Gotoh, SLR-based TRF Contributing to the ITRF2000 project, IVS 2002 General Meeting Proceedings, 300–303, 2002.

[4] Sekido M., H. Takiguchi, Y. Koyama, T. Kondo, R. Haas, J. Wagner, J. Ritakari, S. Kurihara and K. Kokado, Ultra-rapid UT1 measurement by e-VLBI, Earth Planets Space, 60, 8, 865–870, 2008.

UTC(NICT) signal transfer system using optical fibers

Miho Fujieda[1] (*miho@nict.go.jp*),
Motohiro Kumagai[1], **Shigeo Nagano**[1]
and Tadahiro Gotoh[1]

[1] *Space-Time Standards Group*,
National Institute of Information and Communications Technology,
4-2-1 Nukui-Kitamachi, Koganei, Tokyo,
184-8795, Japan

Abstract: We developed the coherent frequency transfer system to UTC(NICT) using optical fibers. The transfer stability reached the 10^{-16} level over 1000 seconds. The coherence of the transferred frequency was confirmed by GPS carrier phase. The frequency transfer using optical fibers to the remote VLBI station has been performed continuously, which signal will be used for the VLBI time transfer.

1. Introduction

Due to the significant progress of optical frequency standards, ultra-stable frequency transfer systems are required [1] - [3]. Not only metrology but also particle accelerators and radio astronomy applications demand low phase-noise frequency dissemination systems [4], [5]. It is difficult for conventional frequency transfers via satellite to enable such dissemination, considering the error sources between the ground station and the satellites [6]. Alternatively, it is thought that frequency dissemination by use of optical fibers may be feasible. Stable RF distribution and optical carrier transfer are both under active study for enabling direct comparisons between optical frequency standards [7] - [11]. Transfer stabilities by both methods are beyond those of traditional transfers. In particular, that of optical carrier transfer reaches the 10^{-17} level at 1 second.

To distribute frequency signals as well as to develop an effective method for clock comparisons, National Institute of Information and Communications Technology (NICT) has studied a frequency dissemination system via optical fiber. Previously, we performed a 1-GHz transfer over the 110-km optical fiber link in Tokyo. To suppress the phase noise accumulated in the fiber link, the combined system with electrical and optical cancellation systems was developed, which enabled us the transfer stability in the 10^{-18} level at an averaging time of 1 day [12]. Secondly, to extend the transmission length, a cascaded system which a 1-GHz and 10-GHz transfer systems were connected in series was developed. We performed the 204-km transfer and confirmed that the stability was degraded by $\sqrt{2}$ in the case two transfer systems were connected [13].

In VLBI stations, a stable frequency source such as a hydrogen maser is necessary. Additionally, VLBI time transfer experiment [14] needs a coherent signal to UTC(NICT) to compare its result with other time transfer methods such as GPS and two-way satellite time and frequency transfer. Because the VLBI station was located apart from the UTC(NICT) system in NICT Koganei headquarters, the UTC(NICT) signal was transferred through the optical fibers buried in NICT. Though the length of the optical fibers was about 1 km, its length fluctuation degraded the signal's stability. To cancel the length fluctuation, we developed a UTC(NICT) transfer system with electrical cancellation system using round-trip optical signal. The system has successfully continued the UTC(NICT) signal transfer for more than three months. The detailed system and performance are described in this report.

2. UTC(NICT) signal transfer system

The UTC(NICT) system exists in the south side across the road in NICT Koganei headquarters. In the north side, there is the VLBI station, where the UTC(NICT) signal was required to perform a time and frequency transfer experiment [14]. The coherent signal to UTC(NICT) was transferred through optical fibers buried in NICT, which length was about 1 km and optical loss was less than 2 dB. The UTC(NICT) signal is available in 5 MHz or 10 MHz and generated from a hydrogen maser, which typical stability is about 3×10^{-13} at an averaging time of 1 s. Figure 1 shows the schematic of the UTC(NICT) signal transfer system. We used the transmission frequency of 1 GHz, where the phase resolution was improved better than that of 10 MHz. The 10-MHz UTC(NICT) signal was converted to 1 GHz using a multiply-by-hundred frequency multiplier, which 1-GHz signal was used as the reference signal in the feedback system to cancel the length fluctuation of optical fibers. On the other hand, a 100-MHz signal from a VCXO was converted to 1 GHz using a multiply-by-ten frequency multiplier. The resultant 1-GHz signal modulated the laser current of a distributed feedback laser with a wavelength of 1.5 μm. As a result, a continuous wave (CW) optical signal with the sidebands detuned by 1 GHz was generated and transferred through a single-mode optical fiber from the local site to the remote site. The local site was co-located with the UTC(NICT) system and the remote site was co-located with the VLBI station. Even if the optical fiber length was only 1

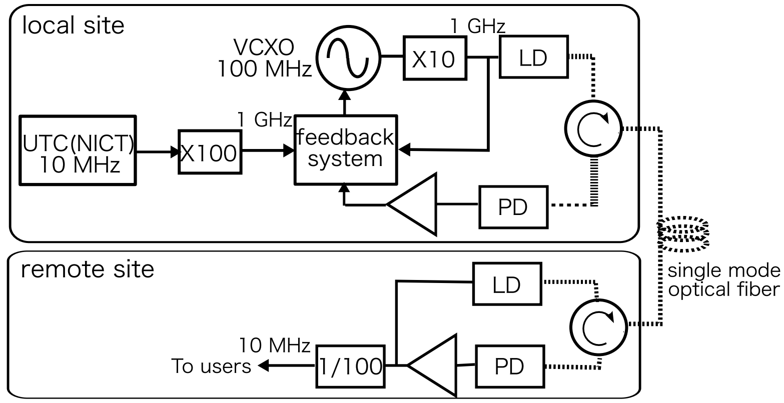

Figure 1. Schematic of UTC(NICT) signal transfer system.

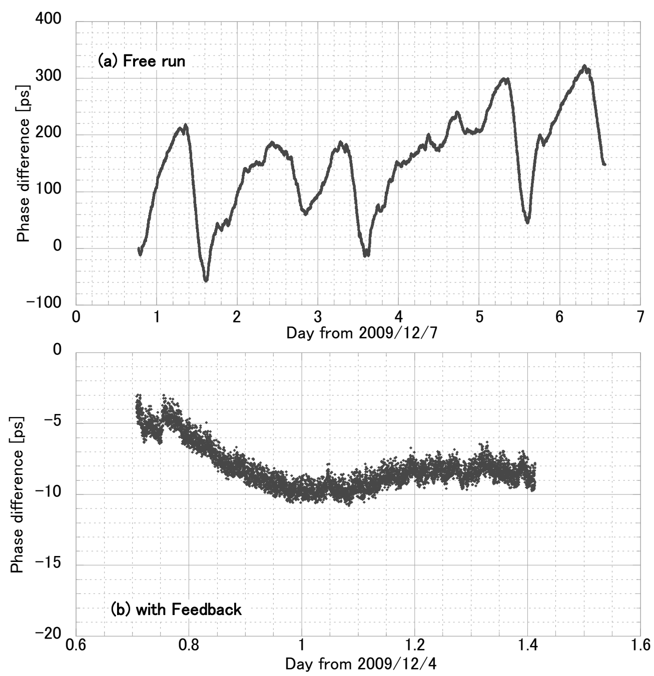

Figure 2. Phase variations of the transferred 10-MHz signal in the cases of free run (a) and with feedback system (b).

km, the length fluctuation of the optical fiber was beyond a few hundred ps in one day. It caused the instability of about 6×10^{-15} at an averaging time of a few hours. It was worse than the stability of the UTC(NICT) and degraded the signal stability transferred to the remote site. To cancel the length fluctuation, the demodulated 1-GHz signal at the remote site modulates the second laser's current. The optical signal was transmitted back to the local site through the same optical fiber. When the feedback system worked at the local site, the error signal was fed back to the VCXO, resulting, the length fluctuation in the transmission path was canceled out and the transferred signal became coherent to the reference signal, that is, UTC(NICT) signal. Concerning to the detail of the feedback system, please refer to [13]. To supply the 10-MHz signal to users, the 1-GHz signal was converted to 10 MHz by a divide-by-hundred prescaler.

To confirm the transfer stability, we installed both of the local and remote systems in the same room and checked the transfer performance using the round-trip optical fibers between the building of UTC(NICT) and VLBI station. Figure 2 shows the phase variations of the transferred 10-MHz signal over the 2-km optical fibers relative to the UTC(NICT) 10-MHz signal, which were measured by a phase comparator every second. Their measurements were performed in the different time.

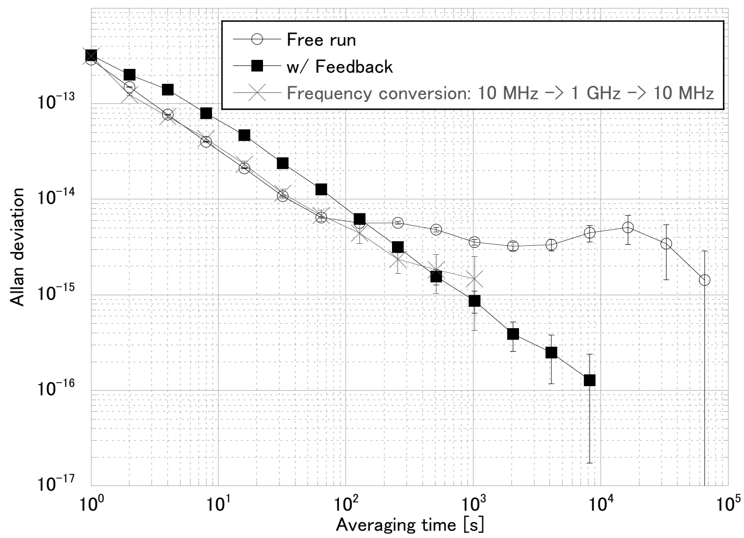

Figure 3. Frequency stabilities of the transferred 10-MHz signal in the cases of free run, with feedback system and frequency conversion between 10 MHz and 1 GHz.

Figure 2 (a) shows the result when the length of the optical fiber was not stabilized by the feedback system and the amplitude of phase variation reached a few hundred ps. On the other hand, (b) shows the result with the stabilization, where the variation decreased less than 10 ps. We can see that a slight phase variation remains there, however. It seems that the transfer system was affected by the variation of the room temperature. Figure 3 shows the frequency stabilities of the transferred 10-MHz signals calculated from the results of Figure 2. The short-term stability at 1 second was limited by the two frequency conversions from 10 MHz to 1 GHz and from 1 GHz to 10 MHz. When the feedback system works, the transfer stability goes down in the 10^{-16} level over 1000 seconds. This stability was good enough for the transfer of UTC(NICT) signal.

Currently, the remote system is co-located with the VLBI station. The signal transfer has continued successfully. The transfer stability was confirmed by frequency transfer using GPS carrier phase. Two GPS receivers were installed in the building of UTC(NICT) system and the VLBI station. Their reference signal were the UTC(NICT) signal and the transferred signal using the optical fibers, respectively. The resultant frequency stability is shown in Figure 4. It proves that the coherence of the transferred signal relative to the UTC(NICT) signal was kept in the 10^{-15} level at 10^4 seconds, which was limited by the performances of the GPS receivers.

3. Summary

To supply the coherent signal to UTC(NICT) to the remote VLBI station, the frequency transfer has been performed over the 1-km optical fibers buried in NICT. The feedback system using the round-trip signal works to cancel the length fluctuation of optical fibers. The system has continuously supplied the coherent signal to UTC(NICT) for more than three months. We confirmed that stable frequency transfer was possible over 200-km urban optical fiber link. Our system would be helpful for users who do not have a stable frequency source.

References

[1] T. Rosenband, D. B. Hume, P. O. Schmidt, C. W. Chou, A. Brusch, L. Lorini, W. H. Oskay, R. E. Drullinger, T. M. Fortier, J. E. Stalnaker, S. A. Diddams, W. C. Swann, N. R. Newbury, W. M. Itano, D. J. Wineland, J. C. Bergquist, "Frequency ratio of Al^+ and Hg^+ single-ion optical clocks; Metrology at the 17^{th} decimal place", *Science*, vol. 319, no. 5871, pp. 1808-1812, 2008.

[2] T. Schneider, E. Peik and Chr. Tamm, "Sub-hertz optical frequency comparisons between two trapped $^{171}Yb^+$ ions", *Phys. Rev. Lett.*, vol. 94, pp. 230801, 2005.

[3] S. Blatt, A. D. Ludlow, G. K. Campbell, J. W. Thomsen, T. Zelevinsky, M. M. Boyd, J. Ye, X. Baillard, M. Fouche, R. Le. Targat, A. Brush,

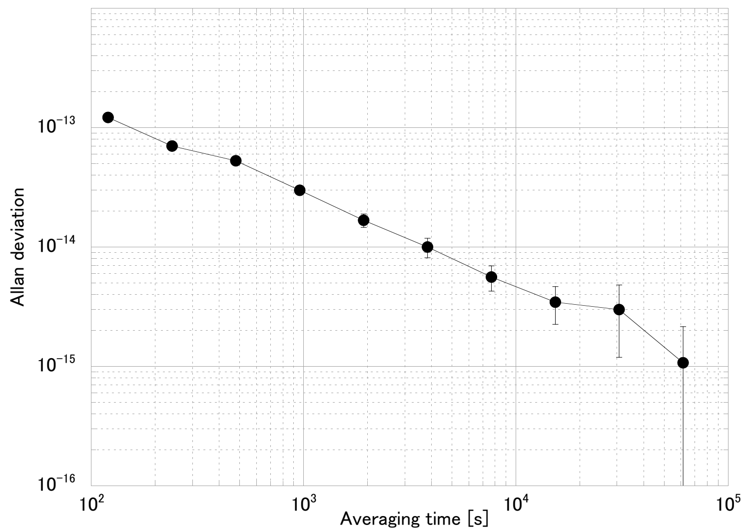

Figure 4. Frequency stabilities between the UTC(NICT) signal and the transferred signal over 1-km optical fiber. The frequency transfer was performed by GPS carrier phase.

P. Lemonde, M. Takamoto, F.-L. Hong, H. Katori, V. V. Flambaum, "New limits on coupling of fundamental constants to gravity using ^{87}Sr optical lattice clocks", *Phy. Rev. Lett.*, vol. 100, pp. 140801, 2008.

[4] J. Frisch, D. Bernstein, D. Brown, and E. Cisneros, "A high stability, low noise RF distribution system", in *Proc. PAC 2002*, vol. 2, pp. 816-818, 2002.

[5] H. Kiuchi, T. Kawanishi, M. Yamada, T. Sakamoto, M. Tsuchiya, J. Amagai, M. Izutsu, "High extinction ratio mach-zehnder modulator applied to a highly stable optical signal generator", *IEEE Trans. Micro. Theo. Tech*, vol. 55, no. 9, pp. 1964-1972, 2007.

[6] A. Bauch, J. Achkar, S. Bize, D. Calonico, R. Dach, R. Hlavac, L. Lorini, T. Parker, G. Petit, D. Piester, K. Szymaniec, P. Uhrich, "Comparison between frequency standards in Europe and the USA at the 10-15 uncertainty level", *Metrologia*, vol. 43, pp. 109-120, 2006.

[7] O. Lopez, A. Amy-Klein, C. Daussy, C. Chardonnet, F. Narbonneau, M. Lours, G. Santarelli, "86-km optical link with a resolution of 2x10^{-18} for RF frequency transfer", *Eur. Phys. J. D*, vol. 48, pp. 35-41, 2008.

[8] P. A. Williams, W. C. Swann, N. R. Newbury, "High-stability transfer of an optical frequency over long fiber-optic links", *J. Opt. Soc. Am. B*, vol. 25, no. 8, pp. 1284-1293, 2008.

[9] M. Musha, F.-L. Hong, K. Nakagawa, K. Ueda, "Coherent optical frequency transfer over 50-km physical distance using a 120-km-long installed telecom fiber network", *Optics Express*, vol. 16, no. 21, pp. 16459-16466, 2008.

[10] G. Grosche, O. Terra, K. Predehl, T. Hansch, R. Holzwarth, B. Lipphard, F. Vogt, U. Sterr, H. Schnatz, "Measurement noise floor for a long-distance optical carrier transmission via fiber", arXiv:0812.0289, 2008.

[11] F. Kefelian, O. Lopez, H. Jiang, C. Chardonnet, A. Amy-Klein, G. Santarelli, "High-resolution optical frequency dissemination on a telecommunications network with data traffic", *Opt. Lett.*, vol. 34, no. 10, pp. 1573-1575, 2009.

[12] M. Kumagai, M. Fujieda, S. Nagano, M. Hosokawa, "Stable radio frequency transfer in 114 km urban optical fiber link", *Optics Letters*, vol. 34, no. 19, pp. 2949-2951, 2009.

[13] M. Fujieda, M. Kumagai, S. Nagano, "Coherent microwave transfer over a 204-km telecom fiber link by a cascaded system", *IEEE TUFFC*, vol. 57, no. 1, pp. 168-174, 2010.

[14] H. Takiguchi, Y. Koyama, R. Ichikawa, T. Gotoh, A. Ishii, T. Hobiger, M. Hosokawa, "VLBI measurements for time and frequency transfer", Proc. of EFTF 2008, 2008.

VLBI Measurements for Frequency Transfer

Hiroshi Takiguchi[1] (*htaki@nict.go.jp*), **Yasuhiro Koyama**[2], **Ryuichi Ichikawa**[1], **Tadahiro Gotoh**[3], **Atsutoshi Ishii**[4], **Thomas Hobiger**[2], **and Mizuhiko Hosokawa**[5]

[1] *Space-Time Standards Group, Kashima Space Research Center, National Institute of Information and Communications Technology, 893-1 Hirai, Kashima, Ibaraki, 314-8501, Japan*
[2] *Space-Time Standards Group, National Institute of Information and Communications Technology, 4-2-1 Nukui-Kitamachi, Koganei, Tokyo, 184-8795, Japan*
[3] *Information Govemance Promotion Team, Information Management Office, National Institute of Information and Communications Technology, 4-2-1 Nukui-Kitamachi, Koganei, Tokyo, 184-8795, Japan*
[4] *Advance Engineering Services Co., Ltd 1-6-1 Takezono, Tsukuba, Ibaraki, 305-0032, Japan*
[5] *New Generation Network Research Center, National Institute of Information and Communications Technology, 4-2-1 Nukui-Kitamachi, Koganei, Tokyo, 184-8795, Japan*

Abstract: We carried out the intercomparison experiment between VLBI and GPS to show that VLBI can measure the correct time difference. We produced an artificial delay change by stretching the Coaxial Phase Shifter which was inserted in the path of the reference signal from Hydrogen maser to the Kashima 11m antenna. Concerning the artificial changes, VLBI and the nominal value of Coaxial Phase Shifter show good agreement, i. e. less than 10ps. Thus it is concluded that the geodetic VLBI technique can measure the time differences correctly.

1. Introduction

As one of the new frequency transfer technique to compare the next highly stable frequency standards, we proposed the geodetic VLBI technique [1], [2]. Previously, we evaluated the ability of VLBI frequency transfer by comparison with GPS carrier phase frequency transfer at Onsala-Wettzell baseline using data from the International VLBI Service for Geodesy and Astrometry (IVS) and the International GNSS Service (IGS). We achieved a frequency stability of 2×10^{-11} at an averaging time of 1 sec following a $1/\tau$ trend. Over the averaging time of 1000 sec, it surpassed the frequency stability of a typical atomic fountain. These results showed that geodetic VLBI technique has the potential for precise frequency transfer [3], [4], [5], [6].

Furthermore, to show the capability of VLBI, we carried out the intercomparison experiments between VLBI and GPS at Kashima 34m - Kashima 11m baseline. In this paper, we describe the comparison with VLBI and GPS carrier phase for that experiment.

2. The intercomparison between VLBI and GPS carrier phase

2.1 Outline of the experiment

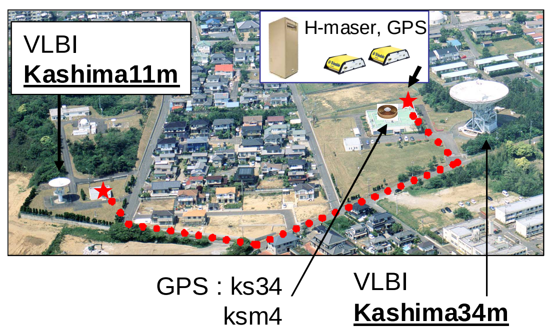

Figure 1. The experimental setup at Kashima station. The baseline length of Kashima 34m - Kashima 11m is about 239m.

Figure 2. The Coaxial Phase Shifter (trombone type) which was made by NIHON KOUSHUHA Co., Ltd. The maximum time change at frequency of 10MHz is 333.7ps.

Figure 1 shows the experimental setup at Kashima station. The baseline length of Kashima

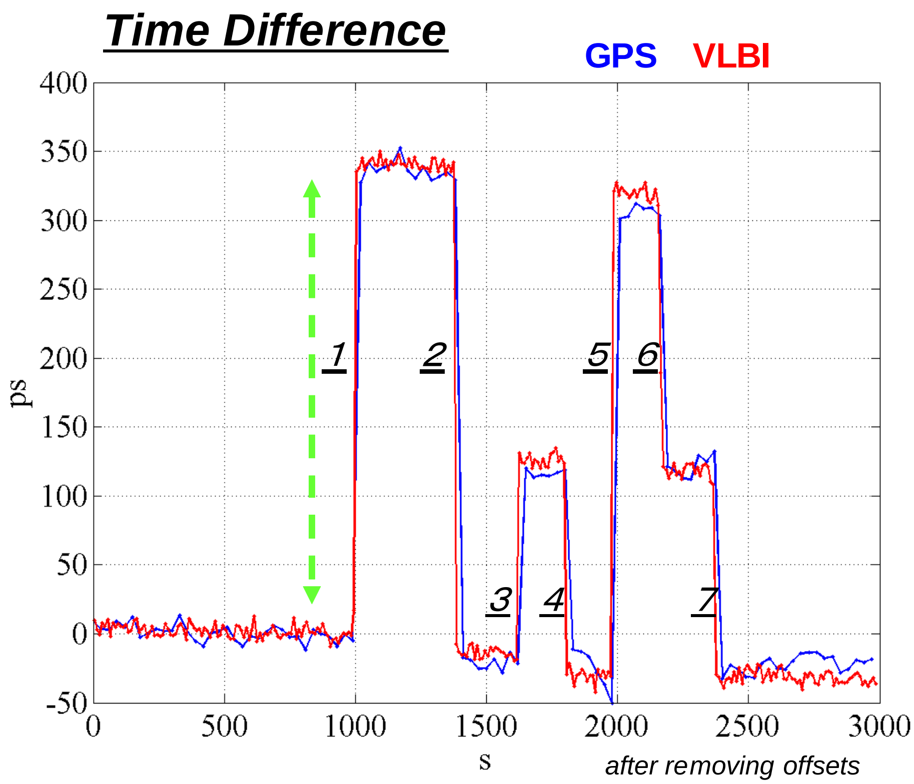

Figure 3. Time difference calculated from VLBI and GPS. The large steps were artificial delay change parts by trombone.

34m - Kashima 11m is about 239m. To produce the artificial delay change, we inserted the Coaxial Phase Shifter (hereafter trombone) (Figure 2) in the signal path of the reference signal from the Hydrogen maser to the Kashima 11m antenna (Figure 4). The trombone can introduce delays in the electrical signal when propagating through the coaxial cable. Thereby, the maximum time change at frequency of 10MHz is 333.7ps.

The outline of the experiment is described in Table 1. We carried out this experiment with a special strategy. Usually, geodetic VLBI observe multiple sources that uniformly cover the sky. And usually clock, atmosphere and station coordinates are estimated with in analysis. However in this experiment, we observed only one source (3C84), and we estimated only clock parameters. We used CALC/SOLVE and Natural Resources Canada's PPP to analyze VLBI and GPS respectively. The details of the data analysis of VLBI and GPS are described in [2].

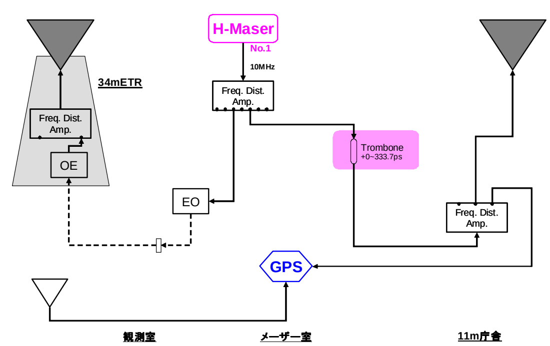

Figure 4. The reference signal setup diagram at Kashima station.

2.2 Results

Figure 3 shows the time difference calculated from VLBI and GPS. The large steps were arti-

Table 1. Difference with the normal geodetic observation

Normal Geodetic VLBI	
Observation	multiple sources
	antenna slew time
	different scan time
	24 hours
Data Analysis	estimate
	clock parameter
	atmosperic delay
	station coordinates
This study	
Observation	one source : 3C84
	no antenna slew time
	same scan time
	a few hours
Data Analysis	estimate only clock parameter
	station coordinates :
	fixed to a-priori coordinates

ficial delay changes introduced by the trombone. Large differences are not seen when comparing in the results between VLBI and GPS.

Table 2 summarizes the differences between nominal value and VLBI, GPS at the artificial delay changes. According to this table, VLBI yields result slightly close to the nominal value than GPS. The results of VLBI and the nominal value of Coaxial Phase Shifter show good agreement, less than 10ps. Anyway, the result of our experiment clearly show that the geodetic VLBI technique can measure the correct time difference.

As already mentioned, this experiment observed only one source continuously. So, we obtained the time difference every 10 seconds from VLBI. Figure 5 shows the frequency stability of VLBI that was calculated from that time difference. The frequency stability reached about the 1×10^{-11} at an averaging time of 1 sec which has an $1/\tau$ trend as in our past research. Also at the averaging time of 500 sec, it surpassed the frequency stability of typical atomic fountain. This averaging time is shorter than our past research.

3. Summary and Outlook

We carried out the intercomparison experiment between VLBI and GPS in order to show that VLBI can measure the correct time difference. We produced artificial delay changes by stretching the trombone which was inserted in the path of the reference signal from Hydrogen maser to Kashima 11m antenna. At the artificial changes, VLBI and the nominal value of trombone show good agreement, less than 10ps. Consequently, the geodetic VLBI technique can measure the correct time difference.

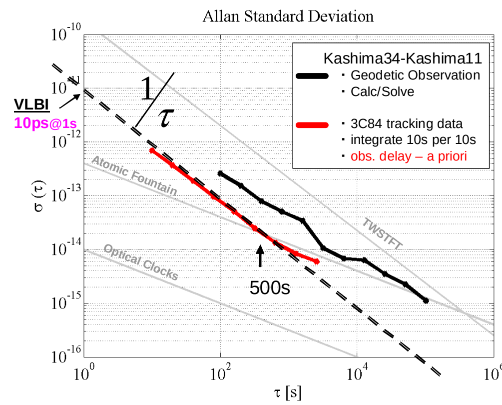

Figure 5. The frequency stability of VLBI that was calculated from the time difference every 10 seconds.

Table 2. The summary of the difference between nominal value and VLBI, GPS at the artificial delay change parts.

	Nominal Value	Nominal-GPS	Nominal-VLBI
1	333.7	3.6	2.8
2	333.7	16.5	15.2
3	147.2	12.8	0.0
4	147.2	17.0	4.6
5	333.7	11.6	19.5
6	186.7	0.6	9.8
7	147.0	9.2	7.3
	mean	10.2	8.5
			ps

NICT has several T&F transfer techniques (Figure 6) other than VLBI such as using GPS and telecommunication satellites at NICT Koganei Headquaters. We set up the TWSTFT (Two-Way Satellite Time and Frequency Transfer) antenna and the Time Comparison Equipment (TCE) ground station of the satellite ETS-VIII (Engineering Test Satellite -VIII) at NICT Kashima Space Research Center (KSRC). KSRC has GPS and VLBI sites. We finished the preparations for exact intercomparison between VLBI and other techniques on the Kashima-Koganei baseline. In the near future, we are going to carry out these intercomparison experiments.

Acknowledgments: The authors would like to acknowledge the IVS and the IGS for the high qual-

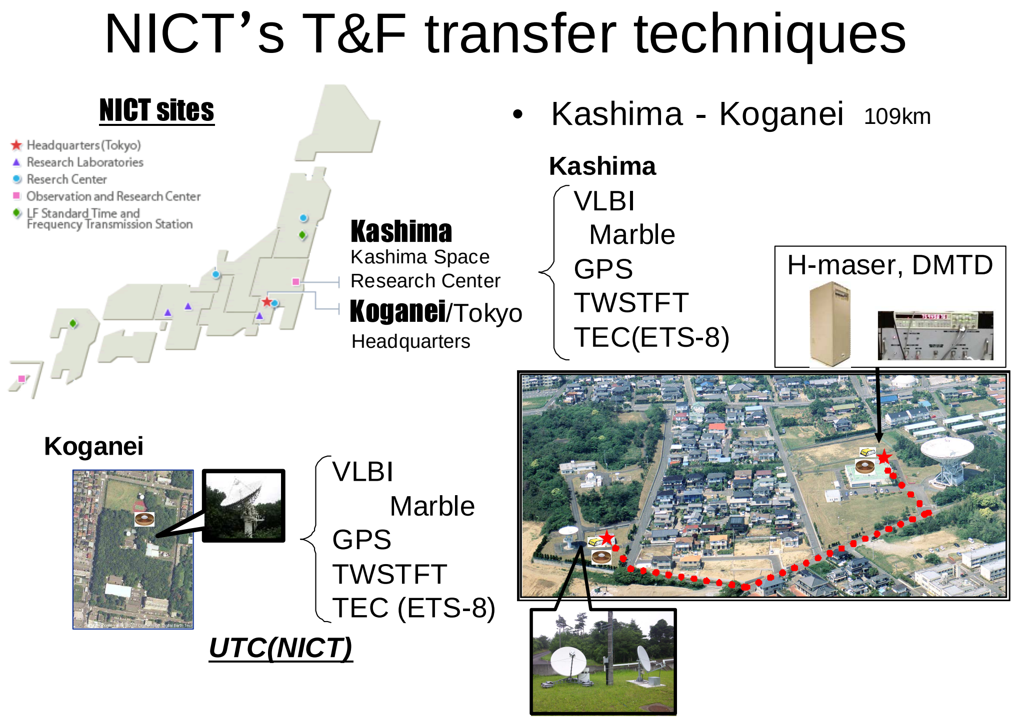

Figure 6. The list and disposition of NICT's T&F transfer techniques.

ity products. We are grateful that GSFC and NR Canada provided the VLBI and GPS analysis software (CALC/SOLVE and NRCan's PPP). The VLBI experiments were supported by M. Sekido and E. Kawai of the Kashima Space Research Center.

References

[1] Koyama, Y., H. Takiguchi, T. Hobiger, and R. Ichikawa, Precise Time Transfer by Means of Geodetic VLBI Technique, *JPGU Meeting 2007 Abstract*, D106-002, 2007.

[2] Takiguchi, H., T. Hobiger, A. Ishii, R. Ichikawa, and Y. Koyama, Comparison with GPS Time Transfer and VLBI Time Transfer, *IVS NICT-TDC News*, No.28, 10–15, 2007.

[3] Takiguchi H., Y. Koyama, R. Ichikawa, T. Gotoh, A. Ishii, T. Hobiger and M. Hosokawa, Comparison Study of VLBI and GPS Carrier Phase Frequency Transfer using IVS and IGS data, *IVS NICT-TDC News*, No.29, 23-27, 2008.

[4] Takiguchi H., Y. Koyama, R. Ichikawa, T. Gotoh, A. Ishii, T. Hobiger and M. Hosokawa, VLBI MEASUREMENTS FOR FREQUENCY TRANSFER, *ATF 2008 Proceedings*, 2008.

[5] Takiguchi H., Y. Koyama, R. Ichikawa, T. Gotoh, A. Ishii, and T. Hobiger, Comparison Study of VLBI and GPS Carrier Phase Frequency Transfer - Part II -, *IVS NICT-TDC News*, No.30, 26-29, 2009.

[6] Takiguchi H., Y. Koyama, R. Ichikawa, T. Gotoh, A. Ishii, T. Hobiger and M. Hosokawa, VLBI Measurements for Frequency Transfer, *Highlights of Astronomy*, 15, 2009.

Kashima RAy-Tracing Service: KARATS

ICHIKAWA Ryuichi[1] (*richi@nict.go.jp*),
Thomas HOBIGER[2],
HASEGAWA Shingo[1],
TSUTSUMI Masanori[1],
KOYAMA Yasuhiro[2],
KONDO Tetsuro[1]

[1] *Kashima Space Research Center, National Institute of Information and Communications Technology, 893-1 Hirai, Kashima, Ibaraki 314-8501, Japan*
[2] *Space-Time Standards Group,National Institute of Information and Communications Technology, 4-2-1, Nukui-Kitamachi, Koganei, Tokyo 184-8795, Japan*

Abstract: The ray tracing tools, which we have named 'KAshima RAytracing Tools (KARAT)', are capable of calculating total slant delays and ray-bending angles considering real atmospheric phenomena. We compared PPP solutions using KARAT with that using the Global Mapping Function (GMF) and Vienna Mapping Function 1 (VMF1) for GPS sites of the GEONET (GPS Earth Observation Network System) operated by Geographical Survey Institute (GSI). Our comparisons show the KARAT solutions are almost identical or slightly better than the solutions using VMF1 and GMF with linear gradient model for horizontal and height positions. In addition we have started the web-base service "KARATS" for reducing atmospheric delay error from the RINEX file.

1. Introduction

We have developed a state-of-art tool to obtain atmospheric slant path delays by ray-tracing through the meso-scale analysis data from numerical weather prediction with 10 km horizontal resolution provided by the Japan Meteorological Agency (JMA)[1, 2]. The tool, which we have named 'KAshima RAytracing Tools (KARAT)', is capable of calculating total slant delays and ray-bending angles considering real atmospheric phenomena. Based on the evaluations of the KARAT performance, we have started the web-based online service, 'KAshima RAytracing Service (KARATS)' for providing the atmospheric delay correction of RINEX files on Jan 27th, 2010. The KARATS receives user's RINEX data via a proper web site (**http://vps.nict.go.jp/karats/index.html**) and processes user's data files. In this short report we describe the recent performance of the KARAT and KARATS service.

2. KARAT and its performance

The KARAT can estimate atmospheric slant delays by three different calculation scheme[2]. These are (1) a piece-wise linear propagation, (2) an analytical 2-D ray-propagation model[3], and (3) a 3-D Eikonal equation. Though the third scheme can include small scale variability of atmosphere in the horizontal component, it has a significant disadvantage due to the massive computational load.

In order to compare KARAT processing and modern mapping functions we analyzed data sets of GEONET, which is a nationwide GPS network operated by GSI. In our comparison 57 stations from GEONET of the year 2008 were considered for processing. We selected the stations which were not affected by crustal deformations caused by seismic activities. Since these 57 stations are distributed over the whole Japan islands evenly, we can investigate effects of various weather conditions on the processing. In addition, we can avoid uncertainties due to the individual difference of equipments in term of the same type of antenna-receiver set in GEONET. The precise point positioning (PPP) processing were carried out using GPSTOOLS[4].

2.1 Monthly Averaged Repeatability

In order to examine the position error magnitude the monthly averaged repetabilities for each coordinate component at both stations are displayed in Figure 1. In this figure five cases of solutions (i.e. Eikonal solver, Thayer model[3], VMF1[5, 7] with gradient[8], VMF1 without gradient, GMF[6] with gradient, and GMF without gradient) are shown. The results of VMF1 without gradient reveal the largest repeatability value for all components at both stations during the summer season (July, August, and September), as one would expect. Tsukuba and Koganei have undergone severe heavy rainfall event during August 26-31, 2008. Especially, the total rainfall around Tsukuba was about 300 mm during these 6 days. The north-south position errors were caused by steep water vapor gradient associated with an EW rain band which lies around both stations. Such large position errors are partly reduced using the modern mapping functions with gradient model. On the other hand, the results of KARAT solutions (both the Eikonal solver and the Thayer model) are much better for the north-south component at the both station during the July and August. These suggest that the both KARAT solutions are quite competitive to the modern mapping functions with gradient model.

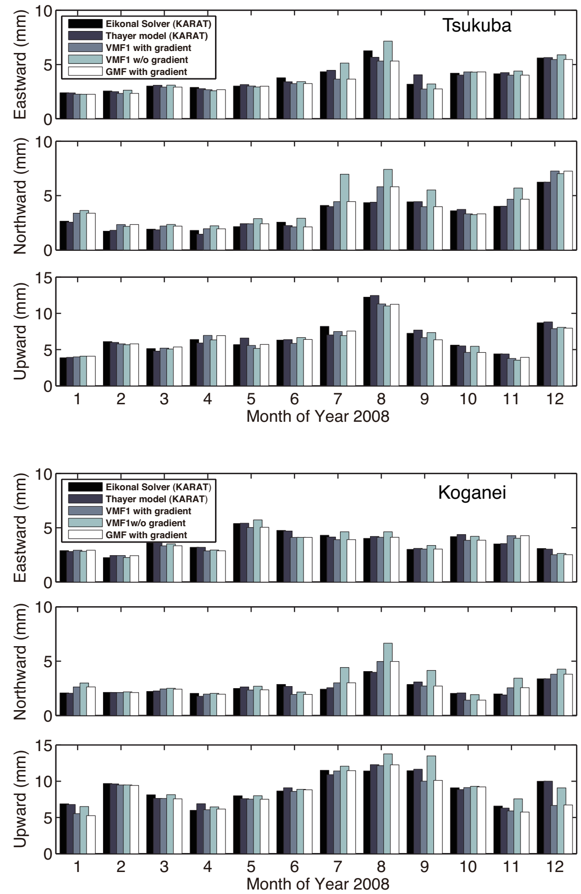

Figure 1. Monthly averaged repeatabilities of station positions at Tsukuba (upper) and Koganei (lower) during year of 2008.

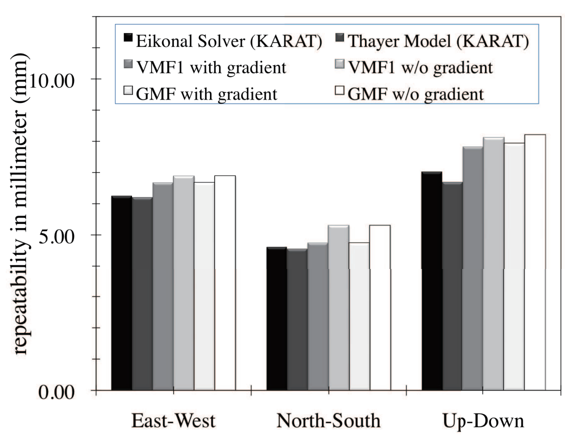

Figure 2. Averaged repeatability of station position during year of 2008 for 57 GEONET stations.

2.2 Yearly Averaged Repeatability

Figure 2 shows the averaged repeatabilities for all 57 stations. In this figure the results for each coordinate component for all six solutions are represented. It indicates that both KARAT solutions are slightly better than the modern mapping functions with gradient solution. However, there are no significant differences between the Eikonal solver and the Thayer model.

2.3 MANAL Scheme Improvement

The grid interval of the MANAL data was updated from 10km to 5km on April 7 2009 (see Figure 3 for example). We have assessed the impacts of data scheme improvement on the KARAT-based PPP solutions by the similar comparison as described above. In this comparison 1214 GEONET stations of the June of year 2009 were processed. The preliminary comparison it is not clear the impact of scheme improvement as shown in Figure 4. The relatively high elevation cut off angle (10 deg.) may cause such results.

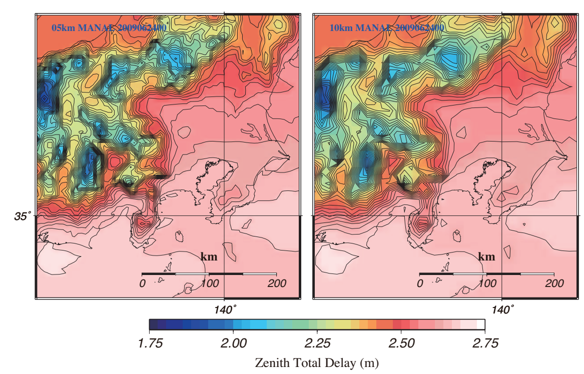

Figure 3. Examples of zenith total delay map on 00UT of June 24th, 2009: 5km MANAL (left) and 10km MANAL (right).

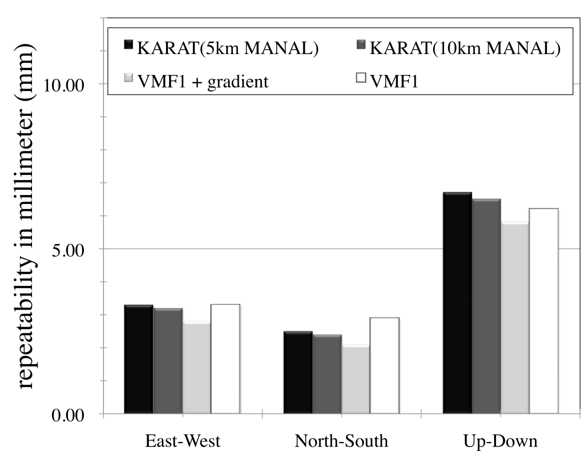

Figure 4. Averaged repeatability of station position during June 2009 for 1214 GEONET stations.

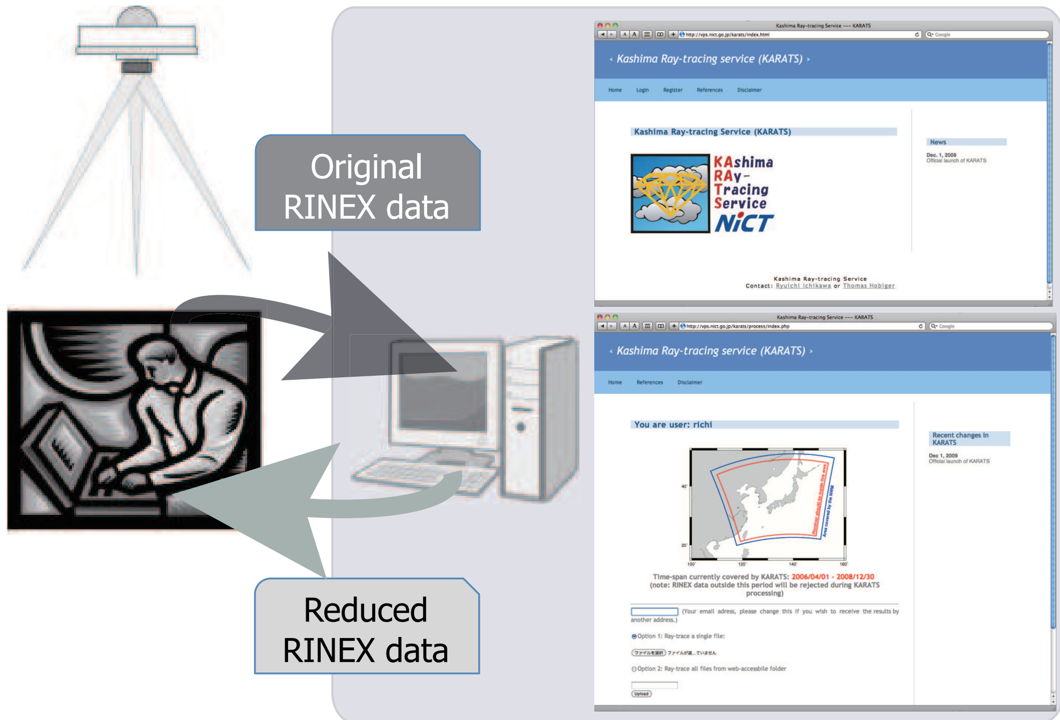

Figure 5. Schematic image of the KARATS. The right upper shows the top page of the KARATS site and the right lower shows the user page.

3. KARATS

On Jan 27th, 2010 we have started the web-based online service "KARATS"(see Figure 5). The KARATS receives user's RINEX data via a proper web site (**http://vps.nict.go.jp/karats/index.html**) and processes user's data files using KARAT for reducing atmospheric slant delays. The reduced RINEX files are archived in the specific directory for each user on the KARATS server. Once the processing is finished the information of data archive and the "kml" file, which shows the user site on the GoogleEarth™(see Figure 6), are sent privately via email to each user. If user want to process a large amount of data files, user can prepare own server which archives them. The KARATS can get these files from the user's server using "GNU wget" and performs ray-traced corrections. At present KARATS online registration has been disabled. If one want to use it, please contact us via email and we will create an user account for you.

4. Summary and Outlook

The KARAT solution is almost identical to the solution using VMF1 (Vienna mapping function 1) with linear gradient model and some cases tends to be slightly better. On the other hand, the impact of the MANAL scheme improvement on KARAT solutions is not clear at present. In addition the scheme improvement of the JMA MANAL data set has no impact on the KARAT processing at present. We have started the web-based online service KARATS (**http://vps.nict.go.jp/karats/index.html**) for providing the atmospheric delay correction of RINEX files on Jan 27th, 2010. One advantage of KARAT is that the reduction of atmospheric path delay will become more accurate each time the numerical weather model are improved (i.e. time and spatial resolution, including new observation data). On October 27, 2009 the JMA started data assimilation of zenith wet delay obtained by the GEONET for meso-scale numerical weather prediction. We are now preparing to evaluate the impacts of the assimilation strategy change on the slant delay reduction.

Acknowledgments: We would like to thank the Geographical Survey Institute, Japan for providing GEONET data sets. We also thank the Japan Meteorological Agency for providing data and products. This study was supported by a Grant-in-Aid for Scientific Research A (No. 21241043) from the Japan Society for the Promotion of Science.

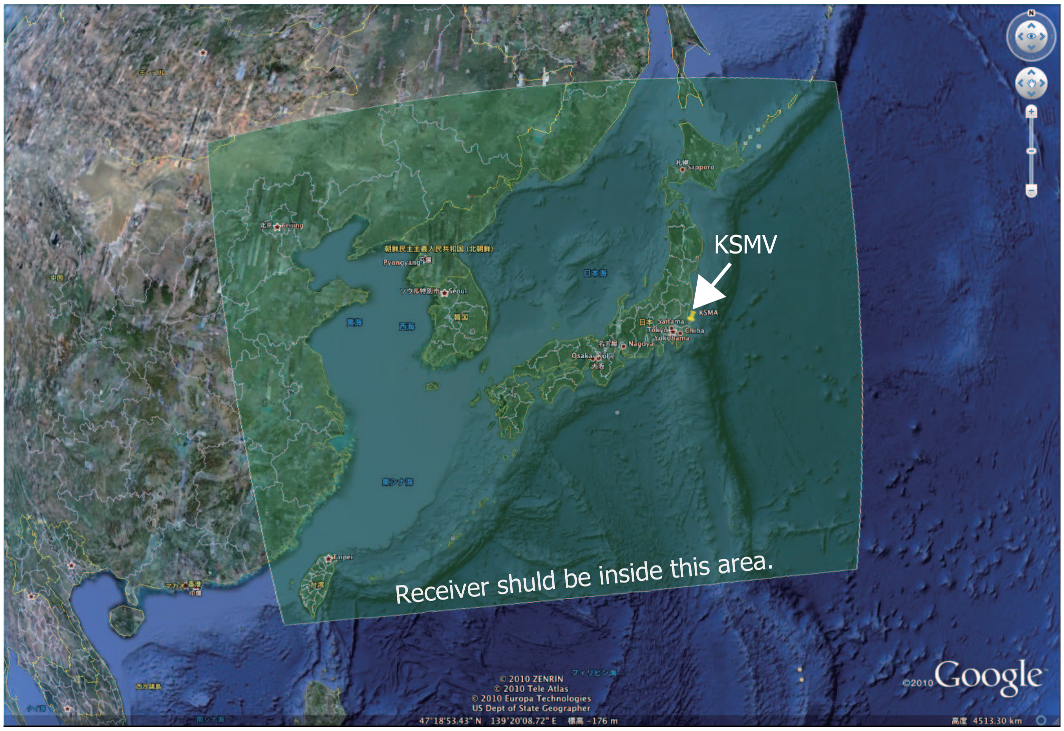

Figure 6. The user's site position shown on the GoogleEarth^{TM}

References

[1] Hobiger, T., Ichikawa R., Takasu T., Koyama Y. and Kondo T., Ray-traced troposphere slant delays for precise point positioning, *Earth Planets Space, 60*, e1–e4, 2008a.

[2] Hobiger, T., Ichikawa R., Koyama Y. and Kondo T., Fast and accurate ray-tracing algorithms for real-time space geodetic applications using numerical weather models, *J. Geophys. Res., 113*, D203027, 1–14, doi:10.1029/2008JD010503, 2008b.

[3] Thayer, G. D., A rapid and accurate ray tracing algorithm for a horizontally stratified atmosphere, *Radio Sci., 1(2)*, 249–252, 1967.

[4] Takasu, T. and Kasai S., Evaluation of GPS Precise Point Positioning (PPP) Accuracy, *IEICE Technical Report, 105(208)*, 40–45, 2005.

[5] Boehm, J. and H. Schuh, Vienna Mapping Functions in VLBI analyses, *Geophys. Res. Lett., 31*, L01603, doi:10.1029/2003GL018984, 2004.

[6] Boehm, J., A. Niell, P. Tregoning, and H. Schuh, Global Mapping Function (GMF): A new empirical mapping function based on numerical weather model data, *Geophys. Res. Lett., 33*, L07304, doi:10.1029/2005GL025546, 2006a.

[7] Boehm, J., B. Werl, and H. Schuh, Troposphere mapping functions for GPS and very long baseline interferometry from European Centre for Medium-Range Weather Forecasts operational analysis data, *J. Geophys.Res., 111*, B02406, doi:10.1029/2005JB003629, 2006b.

[8] MacMillan, D. S., Atmospheric gradients from very long baseline interferometry observations, *Geophys. Res. Lett., 22*, pp.1041–1044, 1995.

"IVS NICT Technology Development Center News" (IVS NICT-TDC News) published by the National Institute of Information and Communications Technology (NICT) (former the Communications Research Laboratory (CRL)) is the continuation of "IVS CRL Technology Development Center News" (IVS CRL-TDC News). (On April 1, 2004, Communications Research Laboratory (CRL) and Telecommunications Advancement Organization of JAPAN (TAO) were reorganized as "National Institute of Information and Communications Technology (NICT)".)

VLBI Technology Development Center (TDC) at NICT is supposed

1) to develop new observation techniques and new systems for advanced Earth's rotation observations by VLBI and other space techniques,
2) to promote research in Earth rotation using VLBI,
3) to distribute new VLBI technology,
4) to contribute the standardization of VLBI interface, and
5) to deploy the real-time VLBI technique.

The NICT TDC newsletter (IVS NICT-TDC News) is published annually by NICT.

This news was edited by Ryuichi Ichikawa and Hiroshi Takiguchi, Kashima Space Research Center, Inquires on this issue should be addressed to H. Takiguchi, Kashima Space Research Center, National Institute of Information and Communications Technology, 893-1, Hirai, Kashima, Ibaraki 314-8501, Japan, TEL : +81-299-84-7133, FAX : +81-299-84-7159, e-mail : htaki@nict.go.jp.

Summaries of VLBI and related activities at the National Institute of Information and Communications Technology are on the Web. The URL to view the home page of the Space-Time Measurement Project of Space-Time Standards Group is :
"http://www.nict.go.jp/w/w114/stmp/index_e.html".

IVS NICT TECHNOLOGY DEVELOPMENT CENTER NEWS No.31, September 2010

International VLBI Service for Geodesy and Astrometry
NICT Technology Development Center News
published by
National Institute of Information and Communications Technology,
893-1, Hirai, Kashima, Ibaraki 314-8501, Japan

NiCT